Int. J. Multiphase Flow Vol. 18, No. 5, pp. 669–689, 1992
Printed in Great Britain

0301-9322/92 $5.00 + 0.00
Pergamon Press Ltd

COMPRESSIBLE FLOW OF A TWO-PHASE FLUID BETWEEN FINITE VESSELS—II

ABEL–NOBLE CARRIER GAS

D. R. CHENOWETH
Applied Mechanics Department, Sandia National Laboratories, Livermore, CA 94551-0969, U.S.A.

S. PAOLUCCI
Department of Aerospace and Mechanical Engineering, University of Notre Dame, Notre Dame, IN 46556-9956, U.S.A.

(*Received 12 July 1991; in revised form 10 March 1992*)

Abstract—The rapid transfer of a mixture consisting of an Abel–Noble (AN) gas and constant density solid particles (or liquid droplets) without phase change is analytically investigated. The two-phase mixture is assumed to remain homogeneous and at equilibrium in a high-pressure supply vessel as well as during the expansion to a finite volume receiver. The physical conditions required for carrier gases to be accurately described by an AN equation of state are given. It is shown that the expanding mixture, or pseudo-fluid, behaves as a modified AN gas which is pseudo-polytropic. Special emphasis is placed on obtaining approximate analytical solutions which are mathematically valid for all parameter ranges of interest. The general sonic flow solution and the subsonic discharge limit represent two of the three cases which admit such approximate solutions. The third case involves subsonic solutions for the single-fluid problem, where initial particle mass fractions in the supply and receiver are the same. All of these special cases are unique in that, when properly non-dimensionalized, they only depend on the mixture ratio of specific heats and the initial mixture volume fraction combining the individual effects of the particles and gas molecules. Numerical results are also given for subsonic finite volume ratio cases, as well as other subsonic cases which show the effects of parameters describing separate particle and gas contributions not present in the three special approximate solutions. The general results show that often the more simple single-fluid solutions can be used to adequately estimate the behavior of more complex cases.

Key Words: homogeneous, equilibrium, two-phase, ideal gas, finite volume, compressible, transfer

1. INTRODUCTION

The carrier gas is described in this work by an Abel–Noble (AN) equation of state (EOS). The compressiblity factor $Z_G = P_G/\rho_G R_G T_G$ for an AN gas is written in terms of the gas density ρ_G and an empirical gas co-density d_G such that $Z_G = (1 - \lambda_G)^{-1}$, where $\lambda_G = \rho_G/d_G$ can be regarded as the volume fraction of molecules in the gas phase. This means that for constant temperature T_G, the AN gas compressibility is linear with pressure $Z_G = 1 + P_G/d_G R_G T_G$, $R_G = 82.06$ atm cm^3/K mol. The AN-EOS accounts for the finite volume occupied by the gas molecules, but it neglects the effects of intermolecular attraction or cohesion forces.

Part I (Chenoweth & Paolucci 1990a) involved results for an ideal carrier gas where $Z_G = 1$, corresponding to cases where $\lambda_G \ll 1$. The results given here are extensions of the non-ideal pure gas results of Chenoweth (1983). It was shown there that if the gas temperature is much greater than the critical gas temperature $T_G \gg T_c$, then most aspects of gas transfer problems are properly described using the AN-EOS. The restriction $T_G \gg T_c$ allows most common gas species, such as N_2, O_2, CO, CO_2 and Ar, to be used as carrier gases at high temperatures. However, for expansions initiated near room temperature the results are valid only for He, Ne, H_2 and their isotopes. The basic reason why the AN-EOS does so well is because the gas sound speed and the PVT behavior are modeled quite well, even though the specific heats at constant pressure and volume (and therefore their ratio also) are equal to the ideal gas values (Chenoweth 1983). Regarding the use of the AN-EOS, it is important to note that experimental values of d_G are significantly more accurate for predicting PVT behavior than those obtained directly via critical property information

using $d_G = 8P_c/R_G T_c$ or corresponding states (involving averages over many gases) $d_G \approx 10P_c/R_G T_c$ (Chenoweth 1983; Hirschfelder *et al.* 1967; van Wylen & Sonntag 1973).

Errors >4% result for $P_G > 100$ atm if an ideal gas EOS is used for He, Ne and H_2. These three gases have empirical co-densities of 0.0935, 0.0775 and 0.0645 mol/cm^3, respectively. In the range $200 \leqslant T_G \leqslant 350$ K and $0 \leqslant P_G \leqslant 1000$ atm, C_{PG} and C_{VG} can exceed their ideal gas limits resulting from the AN approximation by as much as 12% (Chenoweth 1983). On the other hand, their ratio γ_G may exceed its ideal gas value γ_{G_i} by up to 3 and 4.5%, respectively, for Ne and H_2, and decrease as much as 9% for He. However, Chenoweth (1983) has shown that a greatly improved EOS without such large specific heat errors improves pure gas transfer results by only a small fraction of these errors. It is apparent, therefore, that the accurate AN sound speed and PVT descriptions are the dominant effects, whereas the specific heats are either second order or else they involve compensating effects which cancel much of their influence on the results.

It was shown in Part I that for $P = P_G$ (no particle contribution to pressure other than gas volume displacement) and $T = T_G = T_d$ (no thermal lag between phases), the mixture compressibility factor is

$$Z = \frac{P}{\rho R T} = (1-\lambda)^{-1} = \frac{Z_G}{1-\theta} \qquad [1]$$

when a mixture "gas" constant $R = (1-\phi)R_G$ is defined. The combined particle and gas molecule volume fraction contributions, which include non-ideal carrier gas effects, are given by

$$\lambda = \frac{\rho}{d} = \theta + (1-\theta)\lambda_G, \qquad [2]$$

where

$$d = \left[\frac{1-\phi}{d_G} + \frac{\phi}{d_d}\right] \qquad [3]$$

is the mixture co-density, and the particle co-density is just its density, $d_d = \rho_d$. It will be shown that λ is the key parameter in this study. We note that when $\lambda_G \to 0$, $\lambda \to \theta$, and that the particle volume fraction θ is the key parameter in Part I. In some special cases, it is found that λ describes the problem for arbitrary θ and λ_G so long as they are related by [2]. Equations [1]–[3] illustrate that AN gas/particle mixtures also behave like the ideal gas/particle mixtures treated in Part I. However, the present results, with some exceptions, are considerably more complex than those given in Part I.

As in Part I, the mixture is assumed to remain homogeneous and at equilibrium in each stagnant vessel as well as during the expansion process of the flow between vessels, and no attempt is made to define the physical limitations of these restrictions, since these tasks are clearly beyond the scope of the current analysis.

2. GOVERNING EQUATIONS

Only expressions which are significantly modified from Part I (Chenoweth & Paolucci 1990a) are given here. Equations which are the same as in Part I, or can be obtained by means of a symbol change or simple substitution are not repeated, but the differences in the results are described. Furthermore, the nomenclature is the same as in Part I.

2.1. Isentropic relations and mixture sound speed

The isentropic relations given in Part I describing a reversible adiabatic expansion, where the particle mass fraction ϕ, and therefore also the mixture specific heats, are constant for a calorically perfect gas, must be modified when $Z_G \neq 1$. Here

$$T(\rho Z)^{1-\gamma} = C_1, \quad P(\rho Z)^{-\gamma} = C_2, \quad PT^{-\gamma/(\gamma-1)} = C_3, \qquad [4]$$

and C_1, C_2 and C_3 are constants since

$$\rho Z = \frac{\rho_G Z_G}{1-\phi}. \qquad [5]$$

The mixture ratio of specific heat γ is given by [I.9] (denoting [9] in Part I) and figure I.1 (again denoting figure 1 in Part I) in terms of ϕ, δ and γ_G without change. Here δ is the ratio of the heat capacity of the particles to that of the gas at constant pressure. It must be emphasized again that both ϕ and γ remain constant in the expansion region upstream of the minimum flow area, directly as a result of the previous assumptions rather than from any additional restrictions. However, when the initial receiver mass fraction is different from that of the supply, then obviously the receiver mass fraction must change during the transfer and resulting mixing there. Since γ is a constant bounded by unity and γ_G, an ideal carrier gas undergoes a true polytropic expansion process, while the mixture behaves as a modified polytropic fluid because $Z \neq 1$ if $\theta \neq 0$ even when $Z_G = 1$. Similarly, the AN carrier gas with $Z_G \neq 1$ can only be considered as pseudo-polytropic.

The corresponding mixture adiabatic equilibrium sound speed in the low frequency limit for constant ρ_d is

$$a = a_G \left(\frac{Z}{Z_G}\right)\left[\frac{\gamma}{\gamma_G}(1-\phi)\right]^{1/2}, \qquad [6]$$

where $a_G = Z_G a_{G_i}$ and $a_{G_i} = (\gamma_G R_G T_G)^{1/2}$ are the AN and ideal gas sound speeds, respectively. All the mixture sound speed behavior in this limit involving its minimum, and the corresponding particle volume fraction where the minimum occurs, remains unchanged from that given in Chenoweth & Paolucci (1990b). Thus, as in Part I, it is the possible existence of this minimum where $a \ll a_G$, that can greatly reduce transfer times and that makes the analysis which follows so important.

2.2. *End-state expressions*

Since the end-state can be determined under various thermodynamic conditions without the use of any transient information, it often provides valuable insight without much effort. This is particularly true for investigating the parameter dependence of the always present subsonic approach to pressure equilibrium. Also, in some cases the transient process may not be as important as the nature of conditions following the pressure equilibrium.

The final state, where both pressure and thermal equilibrium exist, has the pressure

$$\bar{P}(\infty) = \bar{T}(\infty)\left[\frac{(1+\rho' V')(1-\lambda_{G1}(0))}{1+V'-\lambda_{G1}(0)(1+\rho' V')}\right], \qquad [7]$$

where the definitions of $\bar{T}(\infty)$, $\bar{T}_2(0)$, V' and $\bar{V}_2$ are given in Part I, using subscripts 1 and 2 to denote supply and receiver values and the bar to indicate non-dimensionalization by the corresponding initial supply quantities. The quantity

$$\rho' = \frac{\rho_{G2}(0)}{\rho_{G1}(0)} = \left\{\lambda_{G1}(0) + [1-\lambda_{G1}(0)]\frac{\bar{T}_2(0)}{\bar{P}_2(0)}\right\}^{-1} \qquad [8]$$

is defined so that pressure relations are in their simplest form in terms of the gas molecule volume fraction parameter $\lambda_{G1}(0) = \rho_{G1}(0)/d_G$ initially existing in the supply. This simplification is to be expected because the particles are not contributing to the pressure other than via volume displacement, as accounted for in V' (see [I.25]). The final supply volume fraction

$$\bar{\theta}_1(\infty) = \left\{\lambda_1(0) + [1-\lambda_1(0)]\frac{\bar{T}(\infty)}{\bar{P}(\infty)}\right\}^{-1} \qquad [9]$$

is best expressed in terms of the combined initial supply volume fraction $\lambda_1(0)$. The final receiver volume fraction is then determined by

$$\bar{\theta}_2(\infty) = \bar{\theta}_2(0) + \frac{1-\bar{\theta}_1(\infty)}{\bar{V}_2}, \qquad [10]$$

where

$$\bar{\theta}_2(0) = \left\{\theta_1(0) + \left[\frac{\bar{\phi}_2^{-1}(0)-\phi_1}{1-\phi_1}\right]\left[\lambda_1(0) - \theta_1(0) + [1-\lambda_1(0)]\frac{\bar{T}_2(0)}{\bar{P}_2(0)}\right]\right\}^{-1} \qquad [11]$$

is related to other initial condition parameters.

In the adiabatic limit the supply pressure can be written as

$$\bar{P}_1 = \left[\frac{1-\lambda_1(0)}{\bar{\theta}_1^{-1}-\lambda_1(0)}\right]^{\gamma_1} \qquad [12]$$

and the receiver pressure as

$$\bar{P}_2 = \bar{T}_2\left\{\frac{1-\lambda_1(0)}{\theta_1(0)-\lambda_1(0)+\left(\frac{1-\phi_1}{\bar{\phi}_2^{-1}-\phi_1}\right)[\bar{\theta}_2^{-1}-\theta_1(0)]}\right\}, \qquad [13]$$

while the expressions for $\bar{\theta}_2$, $\bar{\phi}_2$ and $\bar{T}_2$ remain unchanged from Part I (see [I.30]–[I.32], respectively). Therefore, at adiabatic equilibrium, where $\bar{P}_1 = \bar{P}_2$ and $t = t_{eq}$:

$$\bar{P}_1 = \frac{[1-\lambda_1(0)][1+\beta\bar{V}_2\bar{T}_2(0)]}{1+(1+\beta\bar{V}_2)[\theta_1(0)-\lambda_1(0)]+\dfrac{(\beta-\alpha)\bar{V}_2\theta_1(0)\bar{\theta}_1-\{\theta_1(0)-\bar{V}_2[1-\theta_2(0)]\}(1-\bar{\theta}_1+\beta\bar{V}_2)}{1-\bar{\theta}_1+\alpha\bar{V}_2}}. \qquad [14]$$

To define the adiabatic end-state analogous to the isothermal expression $\bar{\theta}_1(\infty)$, [14] must be solved for $\bar{\theta}_1 = \bar{\theta}_1(t_{eq})$. We note that the expressions for α and β are given in Part I (see [I.38] and [I.39]), however, the new expressions for ρ' and $\bar{\rho}_2(0) = \bar{\theta}_2(0)/\bar{\phi}_2(0)$ must be used. In addition, the relations [I.40] and [I.41] between α, β, γ_G, γ_1, ϕ_1, $\bar{\theta}_2(0)$ and $\bar{\phi}_2(0)$ remain unchanged and still dictate the nature of the parameter dependence for various special cases when combined with the new equations just given. Since this parameter dependence is the same as that of the subsonic approach to pressure equilibrium, it is important to briefly review it at this point.

For the general adiabatic problem, the number of parameters is minimized if the following initial data are specified: γ_1, γ_G, $\theta_1(0)$, $\theta_2(0)$, $\bar{P}_2(0)$, $\bar{T}_2(0)$, $\bar{V}_2$ and $\lambda_1(0)$. Then no explicit dependence on $\phi_2(0)$, ϕ_1 or δ_1 is present in the solution of $\bar{\theta}_1(t_{eq})$. That is, the particle volume fraction in the supply vessel at adiabatic pressure equilibrium is independent of ϕ_1 and δ_1, so long as together with γ_G they yield the specified value of γ_1. However, if $\phi_2(0)$ or $\bar{\phi}_2(0)$ is specified as initial data rather than $\theta_2(0)$, then clearly ϕ_1 is also required to determine $\bar{\theta}_2(0)$ and hence the solution $\bar{\theta}_1(t_{eq})$. It should be noted, on the other hand, that the dependence on ϕ_1 is usually weak for $0 < \phi_2(0) < 1$. Two exceptions to this result occur. First, if there are few or no particles initially present in the receiver so that $\bar{\phi}_2(0) \ll 1$ and $\bar{\theta}_2(0) \leqslant 1$, then ϕ_1 and δ_1 do not explicitly influence the end-state solution other than to determine γ_1 via γ_G. Second, if the same fluid present in the supply is initially present in the receiver at a lower pressure so that $\bar{\phi}_2(0) = 1$, then the solution $\bar{\theta}_1(t_{eq})$ depends only on γ_1, $\bar{V}_2$, $\lambda_1(0)$, $\bar{P}_2(0)$ and $\bar{T}_2(0)$; i.e. arbitrary γ_G, ϕ_1, δ_1, $\phi_2(0)$, $\theta_{1}(0)$ and $\lambda_{G1}(0)$ are allowed as long as their combination produce the specified values of γ_1, $\lambda_1(0)$ and $\bar{\phi}_2(0) = 1$. It is clear then that as many as 9 or as few as 6 independent parameters are needed to determine the adiabatic end-state conditions, depending on the nature of the problem and how it is specified.

Some of the limiting solutions of [14] are given in the Appendix, and the following transient results illustrate much of the parameter dependence just outlined.

2.3. *Critical parameters*

The integrated form of the steady, one-dimensional Euler equation, the sound speed expression written in terms of the pressure ratio and therefore the governing equation for the critical pressure ratio $K = P_*/P$, are all exactly the same as given in Part I by [I.43], [I.44] and [I.46], respectively, provided θ_1 is replaced by λ_1 in those equations. Here K, the ratio of the minimum area sonic condition to the stagnant supply pressure, is not constant, as for a pure ideal gas, but changes during the transfer as a function of the supply volume fraction λ_1. The governing expression for K is quadratic in $\lambda_1 = \lambda_1(0)\bar{\theta}_1$ and its solution is

$$\lambda_1 = \frac{\Gamma_1}{1+\Gamma_1}, \qquad [15]$$

where

$$\Gamma_1 = \frac{A+\sqrt{A^2+B}}{\gamma_1 K^{(\gamma_1+1)/\gamma_1}} \qquad [16]$$

and

$$A = 1 - (\gamma_1 + 1)K,\ B = \left(\frac{2\gamma_1^2}{\gamma_1 - 1}\right)\left[1 - \left(\frac{\gamma_1 + 1}{2}\right)K^{(\gamma_1 - 1)/\gamma_1}\right]K^{(\gamma_1 + 1)/\gamma_1}. \quad [17]$$

Equation [15] explicitly relates λ_1 to any K/K_0 for given $1 \leqslant \gamma_1 \leqslant \gamma_G$, as in figure I.4, provided the abscissa in that figure is changed from θ_1 to λ_1, and the $\lambda_1(0) \ll 1$ limit of K is represented by $K_0 = [2/(\gamma_1 + 1)]^{\gamma_1/(\gamma_1 - 1)}$ now. In addition, with the same change of variables, the approximate expression for K/K_0 written as a quadratic equation in λ_1 is given by [I.49]–[I.51], and those expressions are accurate for $\lambda_1 \leqslant 0.6$. Among the related critical ratios given by [I.52], T_*/T_1 and $\rho_* a_*/\rho_1 a_1$ are not altered but a_*/a_1 and $\rho_*/\rho_1 = \theta_*/\theta_1$ are obtained by replacing θ_1 by λ_1; however, a more complex expression for the critical gas to particle density ratio now results:

$$\frac{r_*}{r_1} = \frac{1 - \theta_1}{\lambda_1 - \theta_1 - (1 - \lambda_1)K^{-1/\gamma_1}}. \quad [18]$$

2.4. Transient equations

We assume, as in Part I, that the finite volume reservoirs containing the nearly stagnant homogeneous gas/particle mixtures are joined by a nozzle or an orifice of negligible volume to control the flow. The transfer is treated as quasi-steady in the sense that the steady integrated Euler equation is applied across the flow control region at each instant of time, as in pure gas analyses (Chenoweth 1974, 1983).

Similar to the end-state analysis, useful quantities are easily calculated algebraically once θ_1 or θ_2 is found. The rate of change of the supply volume fraction for the adiabatic case is found to be given by the following non-linear ordinary differential equation:

$$\frac{d\bar{\theta}_1}{d\tau} = -\left(\frac{\bar{V}_2}{1 + \bar{V}_2}\right)\{\lambda_1(0) + [\bar{\theta}_1^{-1} - \lambda_1(0)]y^{-1/\gamma_1}\}^{-1}\left\{\frac{2(1 - \phi_1)}{\gamma_G}\left[\frac{1 - \lambda_1(0)}{\bar{\theta}_1^{-1} - \lambda_1(0)}\right]^{\gamma_1 - 1}\right\}^{1/2}$$
$$\times\left\{\left[\frac{\bar{\theta}_1\lambda_1(0)}{1 - \bar{\theta}_1\lambda_1(0)}\right](1 - y) + \left(\frac{\gamma_1}{\gamma_1 + 1}\right)(1 - y^{1 - 1/\gamma_1})\right\}^{1/2}. \quad [19]$$

The above equation depends on the pressure ratio

$$y = \begin{cases} K & \text{when } \bar{P}_2/\bar{P}_1 \leqslant K, \\ \bar{P}_2/\bar{P}_1 & \text{when } K < \bar{P}_2/\bar{P}_1 \leqslant 1, \end{cases} \quad [20]$$

corresponding to sonic or subsonic exit velocity at the minimum flow area A_e. Here the velocity at A_e has been normalized by the initial ideal gas supply sound speed. Thus, the non-dimensional time is

$$\tau = \left[\frac{A_e a_{G_1}(0)}{V_2}\right](1 + \bar{V}_2)t, \quad [21]$$

and the $\bar{V}_2$ scaling is included to aid in the treatment of the charging $\bar{V}_2 \ll 1$ and discharging $\bar{V}_2 \gg 1$ limits. The differential equation [19] must be integrated from $\tau = 0$, where $\bar{\theta}_1(0) = 1$ to $\tau = \tau_{eq}$ where $\bar{\theta}_1$ approaches the end-state value $\bar{\theta}_1(t_{eq})$. Obviously, $K(\gamma_1, \lambda_1(0)\bar{\theta}_1)$ and $\bar{P}_2/\bar{P}_1$ are required as the integration is performed. The receiver volume fraction is obtained from the relation

$$\bar{\theta}_2 = \bar{\theta}_2(0) + \frac{1 - \bar{\theta}_1}{\bar{V}_2}, \quad [22]$$

so that additional parameters enter from it as well as through the calculation of $\bar{P}_2/\bar{P}_1$.

3. TRANSIENT RESULTS

All solutions of [19] in the limit $\lambda_{G1}(0) \ll 1$ and reported in Part I have been obtained by numerical integration, with the exception of the dilute volume fraction limit $\theta_1(0) \ll 1$. We note that the analytical dilute volume fraction limiting result was easier to understand than the more general numerical solutions because of the reduced number of parameters involved in that case. Here, more

emphasis is placed on analytical approximations valid not only for non-negligible $\lambda_{G1}(0)$, but also non-negligible $\theta_1(0)$ or $\lambda_1(0)$ as well. However, numerical solutions of [19] are still obtained for comparison with the approximate analytical expressions and in cases where no approximate solutions are available.

3.1. Approximate sonic solution

An approximate sonic solution, valid when $\bar{P}_2/\bar{P}_1 \leqslant K$, is obtained upon expanding all terms on the r.h.s. of [19] involving $\bar{\theta}_1$, including y since $y = K(\gamma_1, \lambda_1(0)\bar{\theta}_1)$, for $\lambda_1(0) \ll 1$, and retaining only the linear terms in the integrated result. The constant scaling factor $[1-\lambda_1(0)]^{(\gamma_1-1)/2}$ is not linearized, however. This procedure, although not rigorously justifiable, produces results which are accurate for $\lambda_1(0) \leqslant 0.6$ over the entire range of $1 < \gamma_1 \leqslant 5/3$, and even for larger $\lambda_1(0)$ in narrower ranges of γ_1. This unusual circumstance is apparently due to fortunate off-setting or canceling of higher-order effects. The same procedure with similar results was used by Chenoweth (1983) for a pure AN gas. Mathematically, such behavior simply indicates that the integrands evaluated as described above are nearly linear in $\lambda_1(0)$ over a wide range of this parameter.

The resulting solution is, of course, independent of all receiver parameters including $\bar{V}_2$, $\bar{P}_2(0)$, $\bar{\phi}_2(0)$, $\bar{\theta}_2(0)$ etc., although the time at which it ceases to be valid (unchoking time) does depend on these parameters. This solution for $\bar{\theta}_1$ is given implicitly by

$$\left(\frac{A_e a_{G_i 1}(0)}{V_1 \tau_c}\right) t = [1-\lambda_1(0)]^{(1-\gamma_1)/2}[(\bar{\theta}_1^{(1-\gamma_1)/2}-1)+\sigma(\bar{\theta}_1^{(3-\gamma_1)/2}-1)], \qquad [23]$$

where

$$\sigma = \lambda_1(0)(1-K_0)\left(\frac{\gamma_1-1}{3-\gamma_1}\right)\frac{(\gamma_1+1)^2}{2\gamma_1}. \qquad [24]$$

Note that γ_1 and τ_c, given by [I.9] and [I.60] contain the only effects of finite ϕ_1 and these effects may be present even when $\lambda_1(0) \ll 1$. Also notice that γ_G only enters implicitly through γ_1, τ_c and $a_{G_i 1}(0)$. For finite $\lambda_1(0)$, the term multiplied by σ in [23] causes a linear time scale compression, while the constant scaling factor $[1-\lambda_1(0)]^{(1-\gamma_1)/2}$ causes a non-linear time stretching. For increasing $\lambda_1(0)$, the time scale compression always dominates until $\bar{\theta}_1$ is significantly below 0.15 (a number which decreases with decreasing $\gamma_1 < \gamma_G$) for all $\lambda_1(0) \leqslant 0.6$.

An important point to observe is that since the receiver pressure does not enter in obtaining the sonic solution, $\lambda_1(0)$ is the only volume fraction parameter present. In other words, during sonic flow the individual contributions of gas molecules from $\lambda_{G1}(0)$ and particles from $\theta_1(0)$ to $\lambda_1(0)$ are indistinguishible since only their combined mixture effects enter. Similarly, on the non-dimensional time scale, only the mixture ratio of specific heats γ_1 affects the results. Of course in the pure gas limit, $\theta_1(0) \to 0$ [thus $\lambda_1(0) \to \lambda_{G1}(0)$] and $\bar{\theta}_1 = \bar{\rho}_1$, the solution [23] gives the supply gas density time history. The supply pressure time history in terms of the same parameters is obtained directly by substituting $\bar{\theta}_1 = \{\lambda_1(0) + [1-\lambda_1(0)]\bar{P}_1^{-1/\gamma_1}\}^{-1}$. The receiver particle volume fraction time history involves the additional parameters $\bar{V}_2$ and $\bar{\theta}_2(0)$, since $\bar{\theta}_2(t)$ is obtained by inserting $\bar{\theta}_1 = 1 + \bar{V}_2[\bar{\theta}_2(0) - \bar{\theta}_2]$ into the solution. In the limit $\bar{V}_2 \ll 1$, it is apparent that $\bar{\theta}_1$ no longer changes significantly relative to $\bar{\theta}_2$.

A more complex solution valid only for the isothermal limit $\gamma_1 \to 1$ was given in Part I as [I.89]. In this isothermal limit, the present solution

$$\left[\frac{A_e a_{G_i 1}(0)}{V_1}\left(\frac{1-\phi_1}{\gamma_G}\right)^{1/2}\right] t = -e^{1/2}\ln\bar{\theta}_1 + 2\lambda_1(0)(e^{1/2}-1)(\bar{\theta}_1 - 1) \qquad [25]$$

is simpler and almost as accurate. This solution is analogous to the pure AN gas solution given for the isothermal limit by Chenoweth (1983), except for slightly different scaling constants due to the different boundary conditions used here. In addition, the isothermal results given in figure I.7 with $\theta_1(0)$ as the parameter, are also valid here if the curves are simply relabeled with $\lambda_1(0)$ as the parameter. In figure 1 we give similar results for $\gamma_1 = 7/5$ and $\lambda_1(0) = 0.0$, 0.3 and 0.6. The curves are from the numerical solution of [19]. The symbols are from the very simple approximate sonic solution [23], showing that for all practical purposes we know the solutions are the same for all parameter values of interest.

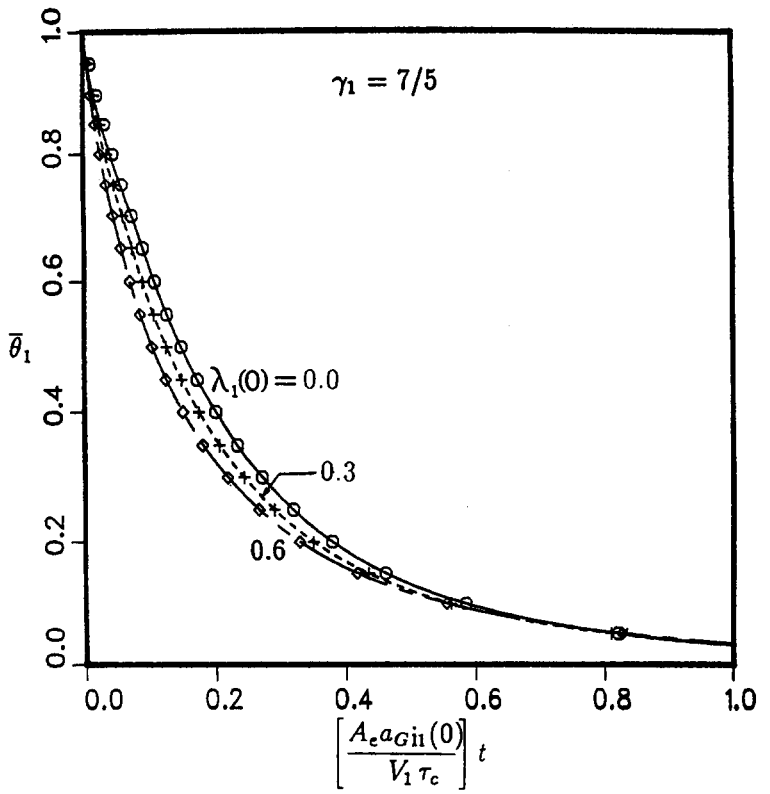

Figure 1. Sonic flow supply particle volume fraction vs reduced time with $\lambda_1(0)$ as the parameter: lines are exact (from [19]), symbols are approximate (from [23]).

3.2. Conditions at end of sonic flow

Since by definition $\bar{P}_1(0) = \bar{\theta}_1(0) = 1$, the sonic flow region will exist initially only if $\bar{P}_2(0) \leqslant K_c \equiv K(\bar{\theta}_1 = 1) = K(\gamma_1, \lambda_1(0))$. On the other hand, a subsonic region will always exist prior to the pressure equilibrium ($\bar{P}_2/\bar{P}_1 = 1$) occurring at $\tau = \tau_{eq}$ if $\bar{P}_2(0) \neq 1$. At the time τ_* when the flow first becomes subsonic, $K = K_* \equiv K(\tau_*)$ and $\bar{\theta}_1 = \bar{\theta}_{1*} \equiv \bar{\theta}_1(\tau_*)$ are obtained by solving the equation $\bar{P}_2/\bar{P}_1 = K$ in the analogous way we obtained the end-state conditions $\bar{\theta}_1 = \bar{\theta}_1(\tau_{eq})$ from solving the equation $\bar{P}_2/\bar{P}_1 = 1$. Although both the sonic and the end-state conditions can be established without detailed knowledge of the transient solution, τ_* and τ_{eq} can only be obtained by integrating the governing equation from $\tau = 0$ until these conditions are reached at $\tau = \tau_*$ and $\tau = \tau_{eq}$, respectively. Also, since the subsonic region is bounded by these two limiting times, it can be expected that both their values depend on the same receiver parameters determined for the special cases in the end-state analysis.

For $\bar{\phi}_2(0) = 1$,

$$\frac{\bar{P}_2}{\bar{P}_1} = \frac{1 - \lambda_1 - \{1 - \lambda_1(0) + \bar{V}_2 \bar{P}_2(0)[1 - \lambda_1(0)\bar{\theta}_2(0)]\}\left[\dfrac{1 - \lambda_1^{-1}}{1 - \lambda_1^{-1}(0)}\right]^{\gamma_1}}{\lambda_1(0) - \lambda_1 - \bar{V}_2[1 - \lambda_1(0)\bar{\theta}_2(0)]} \qquad [26]$$

so that when $\bar{P}_2/\bar{P}_1 = K$ and $\lambda_1 = \lambda_1(\gamma_1, K)$ (see [15]) are substituted, a single exact algebraic expression for $K_* = K_*(\gamma_1, \lambda_1(0), \bar{V}_2, \bar{P}_2(0), \bar{\theta}_2(0))$ is obtained which generally must be solved numerically. Of course $\bar{\theta}_2(0)$ may be eliminated in favor of $\bar{T}_2(0)$ if desired. In addition, we have $\bar{\theta}_{1*} = \lambda_{1*}/\lambda_1(0)$, where $\lambda_{1*} = \lambda_1(\gamma_1, K_*)$. Figure 2 gives K_* normalized by the $\lambda_1(0) \ll 1$ limit K_0 vs $\bar{P}_2(0)$ with $\lambda_1(0)$ as the parameter for four values of $\bar{V}_2$ when $\gamma_1 = 7/5$ and $\bar{T}_2(0) = 1$. It should be noted that the discharging limit $\bar{V}_2 \gg 1$ is actually independent of $\bar{T}_2(0)$ and $\bar{\phi}_2(0)$, so those results are more general than the other three cases. The curves are from the numerical solution outlined above, and the symbols are for the approximations to be discussed below. As expected, and as can be seen in figure 2(a), K_* is independent of $\bar{P}_2(0)$ in the charging limit $\bar{V}_2 \ll 1$, since

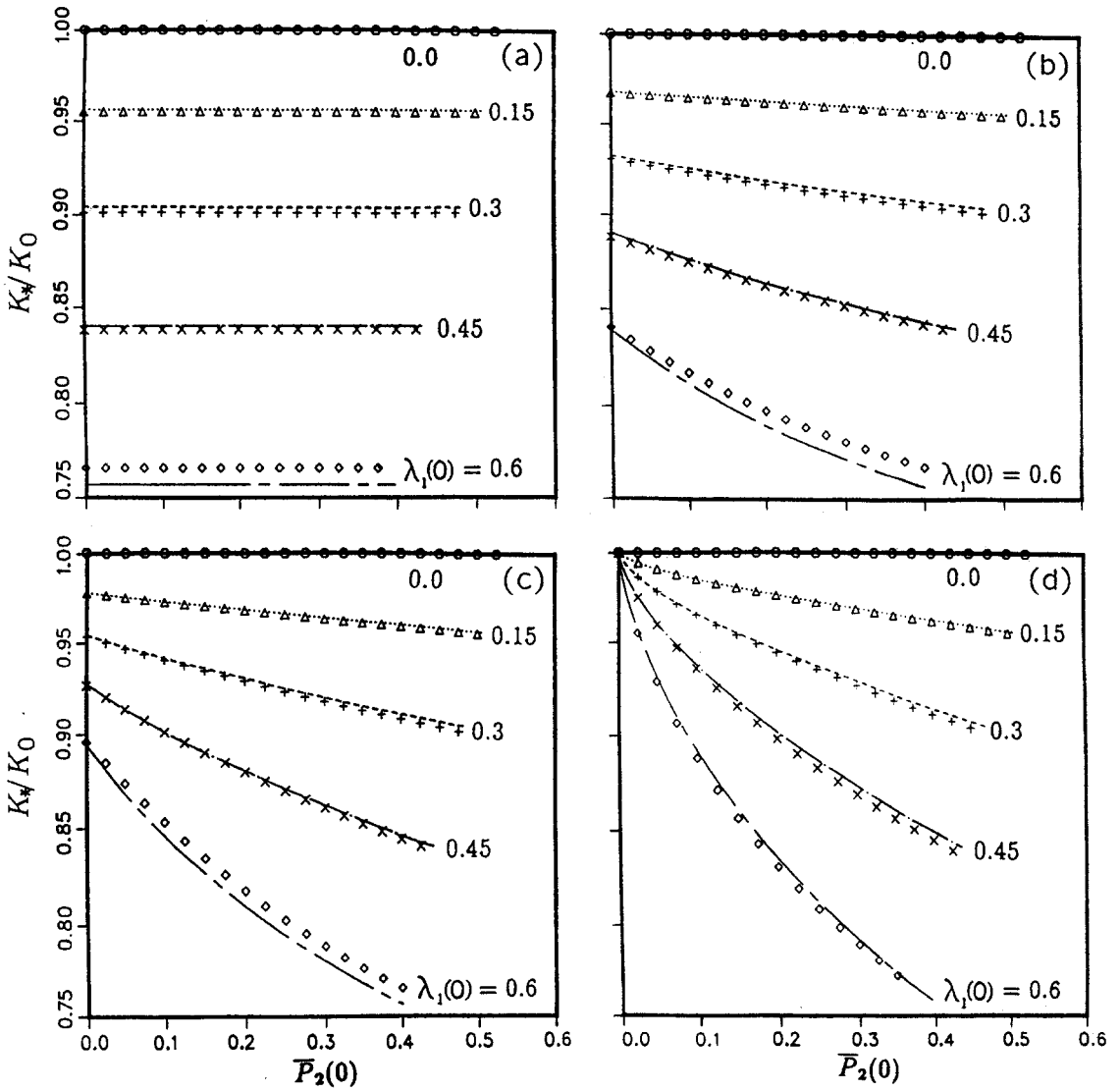

Figure 2. Critical pressure ratio at the end of sonic flow vs initial pressure ratio with $\lambda_1(0)$ as the parameter: lines are exact, symbols are approximate; (a) $\bar{V}_2 \ll 1$, (b) $\bar{V}_2 = 1$, (c) $\bar{V}_2 = 3$, (d) $\bar{V}_2 \gg 1$.

$\bar{\theta}_1 \approx 1$ there and $K_* = K_c = K(\gamma_1, \lambda_1(0))$. For the other values of $\bar{V}_2$, K_* decreases from the vacuum limiting value greater than K_c at $\bar{P}_2(0) = 0$ until it reaches $K_* = K_c = \bar{P}_2(0)$. The corresponding values of τ_*/τ_c are given for the same parameters in figure 3 as the curves obtained by numerical integration until $\bar{P}_2/\bar{P}_1 = K_*$ is reached. Both K_*/K_0 and τ_*/τ_c show increased non-linearity and increased dependence on $\bar{P}_2(0)$ as $\bar{V}_2$ increases and also as $\lambda_1(0)$ increases. In addition, as $\lambda_1(0)$ increases, while the other parameters are fixed, τ_* decreases greatly.

In order to derive approximate analytical solutions valid for subsonic flow which was initially sonic, explicit expressions for τ_* and K_* or $\bar{\theta}_{1*}$ must first be obtained. An accurate expression for τ_* for all cases except $\bar{V}_2 \ll 1$ is obtained using the approximate sonic solution

$$\frac{\tau_*}{\tau_c} = [1 - \lambda_1(0)]^{(1-\gamma_1)/2}[(\bar{\theta}_{1*}^{(1-\gamma_1)/2} - 1) + \sigma(\bar{\theta}_{1*}^{(3-\gamma_1)/2} - 1)](1 + \bar{V}_2^{-1}), \qquad [27]$$

so that only K_* or $\bar{\theta}_{1*}$ is needed from the relation $\lambda_{1*} = \lambda_1(0)\bar{\theta}_{1*} = \lambda_1(\gamma_1, K_*)$. Furthermore, using $\bar{\theta}_1 = 1 + \bar{V}_2[\bar{\theta}_2(0) - \bar{\theta}_2]$ with the sonic solution in the $\bar{V}_2 \ll 1$ limit, we obtain

$$\frac{\tau_*}{\tau_c} = \eta\left[\frac{\bar{\theta}_{2*} - \bar{\theta}_2(0)}{1 - \lambda_1(0)\bar{\theta}_2(0)}\right], \qquad [28]$$

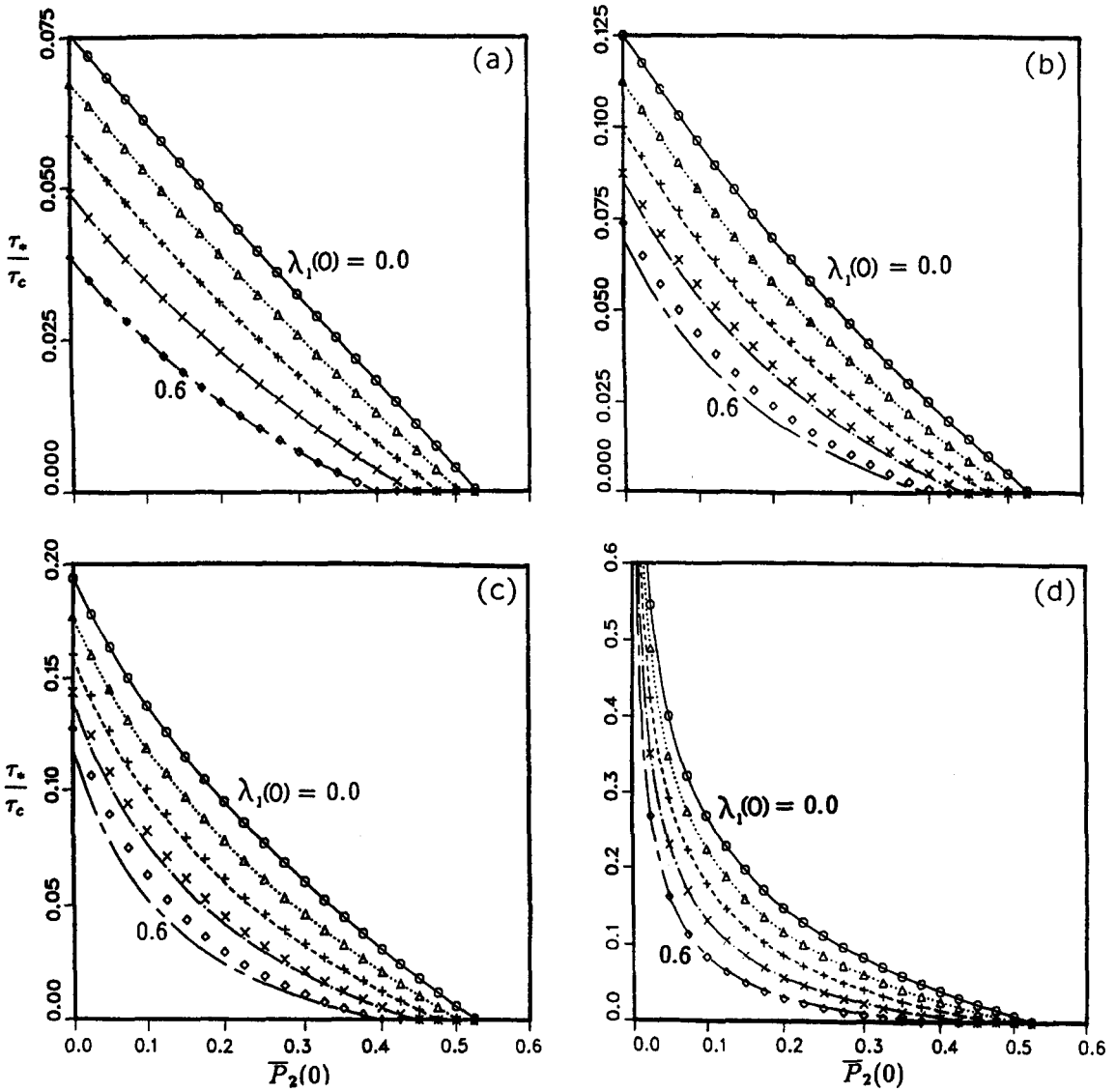

Figure 3. Time of the end of sonic flow vs initial pressure ratio with $\lambda_1(0)$ as the parameter: lines are exact, symbols are approximate; (a) $\bar{V}_2 \ll 1$, (b) $\bar{V}_2 = 1$, (c) $\bar{V}_2 = 3$, (d) $\bar{V}_2 \gg 1$.

where

$$\eta = \left(\frac{\gamma_1 - 1}{2}\right)\left[1 - \sigma\left(\frac{3-\gamma_1}{\gamma_1 - 1}\right)\right][1 - \lambda_1(0)\bar{\theta}_2(0)][1 - \lambda_1(0)]^{(1-\gamma_1)/2}, \qquad [29]$$

so that only $\bar{\theta}_{2*}$ is required in this case. Here, since $\bar{\theta}_{1*} \to 1$, then $K_* = K_c = K(\gamma_1, \lambda_1(0))$. In order to be consistent with the rest of the approximations, it is best to use the explicit expression for K_c written as a quadratic in $\lambda_1(0)$ (see [I.49]), since an approximation of K linear in λ does not have the necessary accuracy for $\lambda_1(0) \leqslant 0.6$.

For the special case $\bar{\phi}_2(0) = 1$, when $\bar{V}_2 \ll 1$

$$\bar{\theta}_{2*} - \bar{\theta}_2(0) = \frac{[K_c - \bar{P}_2(0)][1 - \lambda_1(0)\bar{\theta}_2(0)]}{\gamma_1 + \lambda_1(0)(K_c - 1)}, \qquad [30]$$

so that

$$\frac{\tau_*}{\tau_c} = \eta\left[\frac{K_c - \bar{P}_2(0)}{\gamma_1 + \lambda_1(0)(K_c - 1)}\right] \qquad [31]$$

gives the time where the sonic flow ceases to exist. These results are shown in figures 2(a) and 3(a) by the symbols, with excellent agreement with the more accurate numerical results.

An explicit expression for $\bar{\theta}_{1*}$ which is valid for arbitrary $\bar{V}_2$ can be obtained by equating the $\bar{P}_2/\bar{P}_1$ relation for $\bar{\phi}_2(0) = 1$ to the expansion for K in terms of $\lambda_1 = \lambda_1(0)\bar{\theta}_1$. If we linearize, $\bar{\theta}_{1*}^{-1}$, it is then found that only the linear term in $\lambda_1(0)$ needs to be retained so that

$$\bar{\theta}_{1*}^{-1} = \chi^{1/\gamma_1} - \frac{\lambda_1(0)}{\gamma_1(1+\bar{V}_2K_0)}\left[\left[1-\gamma_1-K_0[1+\bar{V}_2(1-K_0)(1+\gamma_1)]\right.\right.$$
$$\left.\left.+\chi^{1/\gamma_1}\{\gamma_1+K_0+\bar{V}_2K_0[\gamma_1+\bar{\theta}_2(0)]-[1+\bar{V}_2\bar{P}_2(0)\bar{\theta}_2(0)]\chi\}\right]\right], \quad [32]$$

where

$$\chi = \frac{1+\bar{V}_2K_0}{1+\bar{V}_2\bar{P}_2(0)}, \quad [33]$$

can be used to calculate τ_*/τ_c directly from the initial reservoir parameters. The mathematical reason for linearizing the reciprocal of $\bar{\theta}_{1*}$ is easiest to see when the discharging limit $\bar{V}_2 \gg 1$ is extracted from the above expression since then

$$\frac{\bar{P}_2}{\bar{P}_1} = \bar{P}_2(0)\left[\frac{\bar{\theta}_1^{-1}-\lambda_1(0)}{1-\lambda_1(0)}\right]^{\gamma_1} \quad [34]$$

and

$$\bar{\theta}_{1*}^{-1} = \left(\frac{K_0}{\bar{P}_2(0)}\right)^{1/\gamma_1} - \lambda_1(0)\left[\left(\frac{K_0}{\bar{P}_2(0)}\right)^{1/\gamma_1} - (1-K_0)\left(1+\frac{1}{\gamma_1}\right)\right], \quad [35]$$

which produces accurate results valid for all parameter values including $\bar{\phi}_2(0) \neq 1$ [see the symbols in figures 2(d) and 3(d)]. This is due to the fact that $\bar{P}_2(0)$ is the only receiver parameter which appears in the solution in that limit. In addition, figures 3(b) and (c) show good agreement with numerically integrated results when $\bar{V}_2 = 1$ and $\bar{V}_2 = 3$. However, again as for the limit $\bar{V}_2 \ll 1$, the quadratic term in λ_{1*} is required to accurately predict K_* when $\lambda_1(0) \leqslant 0.6$ [see the symbols in figures 2(b) and (c)].

3.3. Approximate subsonic charging solution for $\bar{\phi}_2(0) \equiv 1$

When $\bar{V}_2 \ll 1$, $\bar{\theta}_1 \approx 1$ and $\bar{P}_1 \approx 1$ so that

$$\bar{\theta}_2 - \bar{\theta}_2(0) = [\bar{P}_2 - \bar{P}_2(0)]\left[\frac{1-\lambda_1(0)\bar{\theta}_2(0)}{\gamma_1 - \lambda(0)(1-\bar{P}_2)}\right] \quad [36]$$

and

$$\bar{T}_2 = \frac{\bar{T}_2(0)\bar{P}_2[\gamma_1 - \lambda_1(0)(1-\bar{P}_2(0))]}{\bar{T}_2(0)[1-\lambda_1(0)][\bar{P}_2 - \bar{P}_2(0)] + \bar{P}_2(0)[\gamma_1 - \lambda_1(0)(1-\bar{P}_2)]}, \quad [37]$$

where $\bar{\phi}_2(0) = 1$ and then it follows that

$$\bar{\theta}_2(0) = \left\{\lambda_1(0) + [1-\lambda_1(0)]\frac{\bar{T}_2(0)}{\bar{P}_2(0)}\right\}^{-1}. \quad [38]$$

Obviously, if $\bar{\theta}_2$ or $\bar{P}_2$ is known as a function of time, then these equations determine the entire charging solution.

For example, in this limit when $\bar{\theta}_1 = 1 + \bar{V}_2[\bar{\theta}_2(0) - \bar{\theta}_2]$ is used in the sonic solution

$$\frac{\tau}{\tau_c} = \eta\left[\frac{\bar{P}_2 - \bar{P}_2(0)}{\gamma_1 - \lambda_1(0)(1-\bar{P}_2)}\right], \quad [39]$$

which is valid for $\bar{P}_2 \leqslant K_c$ and η is given by [29]. Here $K_c = K(\bar{\theta}_1 = 1)$ is given by figure I.4 with θ_1 replaced by $\lambda_1(0)$ and γ_1 as the parameter, or figure 2(a) for $\gamma_1 = 7/5$. The quadratic approximation for $K(\gamma_1, \lambda_1)$ from [I.49] is consistent with the approximations being used here and allows explicit calculations.

The corresponding subsonic solution valid for $K_c < \bar{P}_2 \leqslant 1$ is obtained as in Part I via a variable w using

$$y = \bar{P}_2 = (1 - w^2)^{\gamma_1/(\gamma_1 - 1)}. \quad [40]$$

This variable w is bounded by $0 \leqslant w < w_0$ and it is the minimum flow area Crocco number (Chenoweth 1974, sect. D). Physically w represents the fraction of the total enthalpy converted into kinetic energy at that point. The subscript 0 identifies the starting subsonic conditions defined by

$$w_0 = \begin{cases} w_* \equiv (1 - K_c^{(\gamma_1 - 1)/\gamma_1})^{1/2} & \text{if } \bar{P}_2(0) \leqslant K_c, \\ [1 - \bar{P}_2(0)^{(\gamma_1 - 1)/\gamma_1}]^{1/2} & \text{if } \bar{P}_2(0) > K_c, \end{cases} \quad [41]$$

where the related non-dimensional time is

$$\tau_0 = \begin{cases} \tau_* & \text{if } \bar{P}_2(0) \leqslant K_c, \\ 0 & \text{if } \bar{P}_2(0) > K_c. \end{cases} \quad [42]$$

Here τ_*/τ_c is given by [31] and figure 3(a) for $\gamma_1 = 7/5$ and $\bar{T}_2(0) = 1$. The non-dimensional time in this limit becomes

$$\tau = \left(\frac{A_e a_{G_1 1}(0)}{V_2}\right) t, \quad [43]$$

so using [40], [19] can be integrated analytically for small $\lambda_1(0)$ to give

$$\tau = \tau_0 + \tau_w \left[(w_0 - w) \left\{ 1 - \lambda_1(0) \left(\frac{\gamma_1 - 2}{\gamma_1} \right) - \lambda_1(0)[F(w_0) - F(w)] \right\} \right], \quad [44]$$

where similar to the sonic case, only linear first-order dependence on $\lambda_1(0)$ is retained while the integrals are evaluated. The scaling constant τ_w is not linearized, however,

$$\frac{\tau_w}{\tau_c} = \left[\frac{\gamma_1 - 1}{2} K_0^{(\gamma_1 + 1)/\gamma_1} \right]^{1/2} \left[1 - \lambda_1(0) \left\{ \bar{\theta}_2(0) + \left(\frac{1 - \bar{P}_2(0)}{\gamma_1} \right) [1 - \lambda_1(0)\bar{\theta}_2(0)] \right\} \right], \quad [45]$$

with τ_c given by [I.60]. The function $F = F(w)$ is given by

$$F(w) = \left(\frac{\gamma_1 - 1}{2\gamma_1} \right) \left\{ w^{-1}[(1 - w^2)^{(2\gamma_1 - 1)/(\gamma_1 - 1)} - 1] + \left[\frac{3(\gamma_1 + 1)}{3\gamma_1 - 1} \right] w(1 - w^2)^{\gamma_1/(\gamma_1 - 1)} + \left[\frac{8\gamma_1}{(\gamma_1 - 1)(3\gamma_1 - 1)} \right] I_{m/2}(w) \right\} \quad [46]$$

in terms of the integral

$$I_{m/2}(w) = \int (1 - w^2)^{m/2} \, dw = (1 + m)^{-1}[w(1 - w^2)^{m/2} + m I_{m/2 - 1}(w)]. \quad [47]$$

Here $m = 2/(\gamma_1 - 1)$, so that $1 < \gamma_1 \leqslant 5/3$ corresponds to $\infty > m \geqslant 3$. Since $I_{-1/2} = \sin^{-1} w$ and $I_0 = w$, then the integrals $I_{m/2}$ can be evaluated in closed form recursively using these terminators for integer values of $m \geqslant 3$ or $\gamma_1 = 5/3, 6/4, 7/5, 8/6, \ldots$. These values of γ_1 yield closed-form charging solutions when $\lambda_1(0) \neq 0$. These requirements did not exist in Part I, where $\lambda_1(0) = \theta_1(0) \ll 1$ was the only charging solution given for similar approximations. Note that (from [44]) when $\lambda_1(0) = 0$, $F(w)$ and subsequently $I_{m/2}(w)$ are not required. When $\lambda_1(0) \neq 0$, $I_{m/2}$ introduces only polynomials in w of degree $m + 1$ for m even, but it is always transcendental for m odd.

The end-state solution given in the Appendix for this limit is reached at pressure equilibrium $\bar{P}_2 = 1$, where $w = 0$. The time at which this adiabatic pressure equilibrium occurs is obtained by noting that $F(w) \to 0$, so that

$$\tau_{eq} = \tau_0 + \tau_w \left\{ w_0 \left[1 - \lambda_1(0) \left(\frac{\gamma_1 - 2}{\gamma_1} \right) \right] - \lambda_1(0) F(w_0) \right\} \quad [48]$$

and then the transient solution can be expressed as

$$\tau = \tau_{eq} - \tau_w \left\{ w \left[1 - \lambda_1(0) \left(\frac{\gamma_1 - 2}{\gamma_1} \right) \right] - \lambda_1(0) F(w) \right\}. \quad [49]$$

Although this is not an explicit solution for $w(\tau)$ or $\bar{P}_2(\tau)$, using [40] allows τ to be calculated directly for any γ_1, $\bar{P}_2$, $\lambda_1(0)$, $\bar{P}_2(0)$ and $\bar{T}_2(0)$ or $\bar{\theta}_2(0)$. The end-state solution which this solution approaches as $\tau \to \tau_{eq}$ is not an approximation for small $\lambda_1(0)$ and furthermore, it is also *exact* for all values of $1 \leqslant \gamma_1 \leqslant 5/3$, since it is derived without use of the transient solution.

Results for the case when $\gamma_1 = 7/5$ and $\bar{T}_2(0) = 1$ are given in figures 4(a) and (c), where the symbols are from approximations [48] and [49] with definitions [36] and [40] and the curves are from the numerical integration of [19]. Surprisingly, just as for the sonic solution, the small $\lambda_1(0)$ approximation is actually valid for values as large as 0.6. Figure 4(a) gives τ_{eq}/τ_c vs $\bar{P}_2(0)$ for $\lambda_1(0) = 0$, 0.15, 0.3, 0.45 and 0.6. These results include initially sonic as well as initially subsonic cases. The corresponding results for $\bar{\theta}_2 - \bar{\theta}_2(0)$ vs τ/τ_{eq} are given in figure 4(c) for the case where $\bar{P}_2(0) = 1/2$. It is obvious that more error occurs in τ_{eq}/τ_c than in the transient solution in terms of τ/τ_{eq}. When $\lambda_1(0)$ is large, more errors occur for cases which are initially sonic than for cases which are initially subsonic.

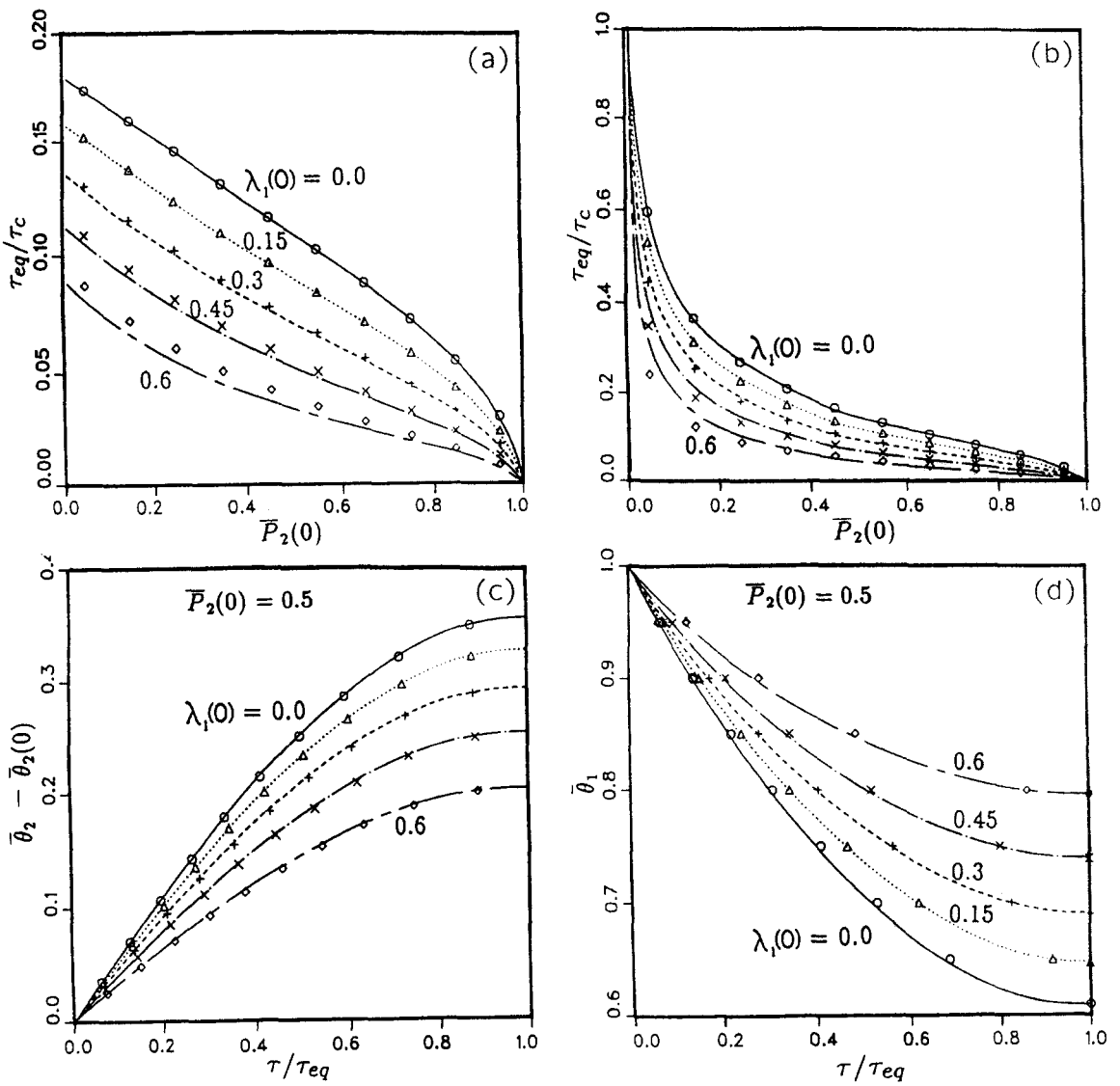

Figure 4. Charging and discharging solutions: lines are exact, symbols are approximate. Time of adiabatic pressure equilibrium vs initial pressure ratio with $\lambda_1(0)$ as the parameter: (a) $\bar{V}_2 \ll 1$, (b) $\bar{V}_2 \gg 1$. Particle volume fraction vs reduced time with $\lambda_1(0)$ as the parameter: (c) $\bar{V}_2 \ll 1$, (d) $\bar{V}_2 \gg 1$.

3.4. Approximate subsonic discharging solution

When $\bar{V}_2 \gg 1$, $\bar{P}_2 \approx \bar{P}_2(0)$, $\bar{\theta}_2 \approx \bar{\theta}_2(0)$ and $\bar{T}_2 \approx \bar{T}_2(0)$, so that

$$\frac{\bar{P}_2}{\bar{P}_1} \approx \bar{P}_2(0)\left[\frac{\bar{\theta}_1^{-1} - \lambda_1(0)}{1 - \lambda_1(0)}\right]^{\gamma_1} \tag{50}$$

and the resulting solution will be valid for all $\bar{\phi}_2(0)$ values because $\bar{P}_2(0)$ is the only receiver parameter which enters the solution. Since $\bar{\lambda}_1 = \bar{\rho}_1 = \bar{\theta}_1$ and $\bar{T}_1 = \bar{P}_1^{(\gamma_1 - 1)/\gamma_1}$, the entire transient solution follows immediately once $\bar{\theta}_1$ is found. This has already been done for the sonic portion of the discharge via that approximate solution.

The related subsonic solution is obtained for $K_* < y \leqslant 1$ as in Part I via a variable z using

$$y = (1 + z^2)^{\gamma_1/(1-\gamma_1)}. \tag{51}$$

The new variable z is bounded by

$$0 \leqslant z \leqslant z_0, \tag{52}$$

and it is proportional to the minimum area Mach number (Chenoweth 1974, sect. E). The subscript 0 identifies the starting subsonic condition defined by

$$z_0 = \begin{cases} z_* \equiv [K_*^{(1-\gamma_1)/\gamma_1} - 1]^{1/2} & \text{if } \bar{P}_2(0) \leqslant K_*, \\ [\bar{P}_2(0)^{(1-\gamma_1)/\gamma_1} - 1]^{1/2} & \text{if } \bar{P}_2(0) > K_*, \end{cases} \tag{53}$$

where the corresponding non-dimensional time is

$$\tau_0 = \begin{cases} \tau_* & \text{if } \bar{P}_2(0) \leqslant K_*, \\ 0 & \text{if } \bar{P}_2(0) > K_*. \end{cases} \tag{54}$$

Here τ_*/τ_c is given by [27] and [35] as well as shown in figure 3(d) for $\gamma_1 = 7/5$. Figure 2(d) gives the related K_* for $\gamma_1 = 7/5$. The non-dimensional time in this limit becomes

$$\tau = \left(\frac{A_e a_{G_i 1}(0)}{V_1}\right) t, \tag{55}$$

so that with [51], [19] can be integrated for small $\lambda_1(0)$ to give

$$\tau = \tau_0 + \tau_z\{[1 + 2\lambda_1(0)][J_{n/2}(z_0) - J_{n/2}(z)] + \lambda_1(0)\bar{P}_2(0)^{1/\gamma_1}[G(z) - G(z_0)]\}, \tag{56}$$

where, as in the sonic case, only linear first-order dependence on $\lambda_1(0)$ is retained in the evaluation of the integrals; as before, however, the scaling constant τ_z is not linearized,

$$\frac{\tau_z}{\tau_c} = \left(\frac{\gamma_1 - 1}{2}\right)^{1/2} K_0^{(\gamma_1+1)/2\gamma_1} \bar{P}_2(0)^{(1-\gamma_1)/2\gamma_1}[[1 - \lambda_1(0)]\{1 - \lambda_1(0)[1 - \bar{P}_2(0)^{1/\gamma_1}]\}], \tag{57}$$

with τ_c as given by [I.60]. The function $G = G(z)$ is

$$G(z) = \frac{2(\gamma_1^2 - 1)}{\gamma_1(5 - \gamma_1)}\left[z(1 + z^2)^{(3-\gamma_1)/(\gamma_1-1)} + \frac{2(3 - \gamma_1)}{(\gamma_1 - 1)} J_n(z)\right] + \left(\frac{\gamma_1 - 1}{2\gamma_1}\right)\left\{z^{-1}(1 + z^2)^{1/(\gamma_1-1)}[1 - (1 + z^2)^{1/(\gamma_1-1)}] - \frac{3 - \gamma_1}{\gamma_1 - 1} J_{n/2}(z)\right\}, \tag{58}$$

in terms of the integrals J_n and $J_{n/2}$, defined by

$$J_n(z) = \int (1 + z^2)^n \, dz = (1 + 2n)^{-1}[z(1 + z^2)^n + 2nJ_{n-1}(z)]. \tag{59}$$

Here

$$n = m - 2 = \frac{2(2 - \gamma_1)}{\gamma_1 - 1}, \tag{60}$$

so that $1 < \gamma_1 \leqslant 5/3$ corresponds to $\infty > n \geqslant 1$. Since $J_{-1/2} = \sinh^{-1} z$ and $J_0 = z$, then the resulting discharging integrals $J_{n/2}$ and J_n can be evaluated recursively in closed form for integer values of $n \geqslant 1$ corresponding to $\gamma_1 = 5/3, 6/4, 7/5, 8/6, \ldots$. Notice that here only the J_n integrals drop out

for $\lambda_1(0) \ll 1$, so that the restriction on γ_1 giving closed-form results remains via $J_{n/2}$ even when low pressure dilute mixtures are discharged. When $\lambda_1(0) \neq 0$, J_n always introduces polynomials in z of degree $2n+1$, but $J_{n/2}$ introduces polynomials of degree $n+1$ only for n even, and it always has logarithmic and square root behavior when n is odd. The end-state solution for this limit is given in the Appendix, and it is valid for all values of $1 \leqslant \gamma_1 \leqslant 5/3$ with no restriction on $\lambda_1(0)$.

At pressure equilibrium $\bar{P}_1 \to \bar{P}_2(0)$, $z \to 0$ and $J_{n/2} \to J_n \to 0$, so that the time required to reach adiabatic pressure equilibrium is

$$\tau_{eq} = \tau_0 + \tau_z\{[1 + 2\lambda_1(0)]J_{n/2}(z_0) - \lambda_1(0)\bar{P}_2(0)^{1/\gamma_1}G(z_0)\} \quad [61]$$

and the related transient solution can be expressed as

$$\tau = \tau_{eq} - \tau_z\{[1 + 2\lambda_1(0)]J_{n/2}(z) - \lambda_1(0)\bar{P}_2(0)^{1/\gamma_1}G(z)\}. \quad [62]$$

Results are given for this case in figures 4(b) and (d) for $\gamma_1 = 7/5$, where the symbols are from approximations [61] and [62] with definitions [50] and [51] and the curves are from the numerical integration of [19]. Again the small $\lambda_1(0)$ approximation is valid for values as large as 0.6. Figure 4(b) gives τ_{eq}/τ_c vs $\bar{P}_2(0)$ for $\lambda_1(0) = 0$, 0.15, 0.3, 0.45 and 0.6. These results include both initially

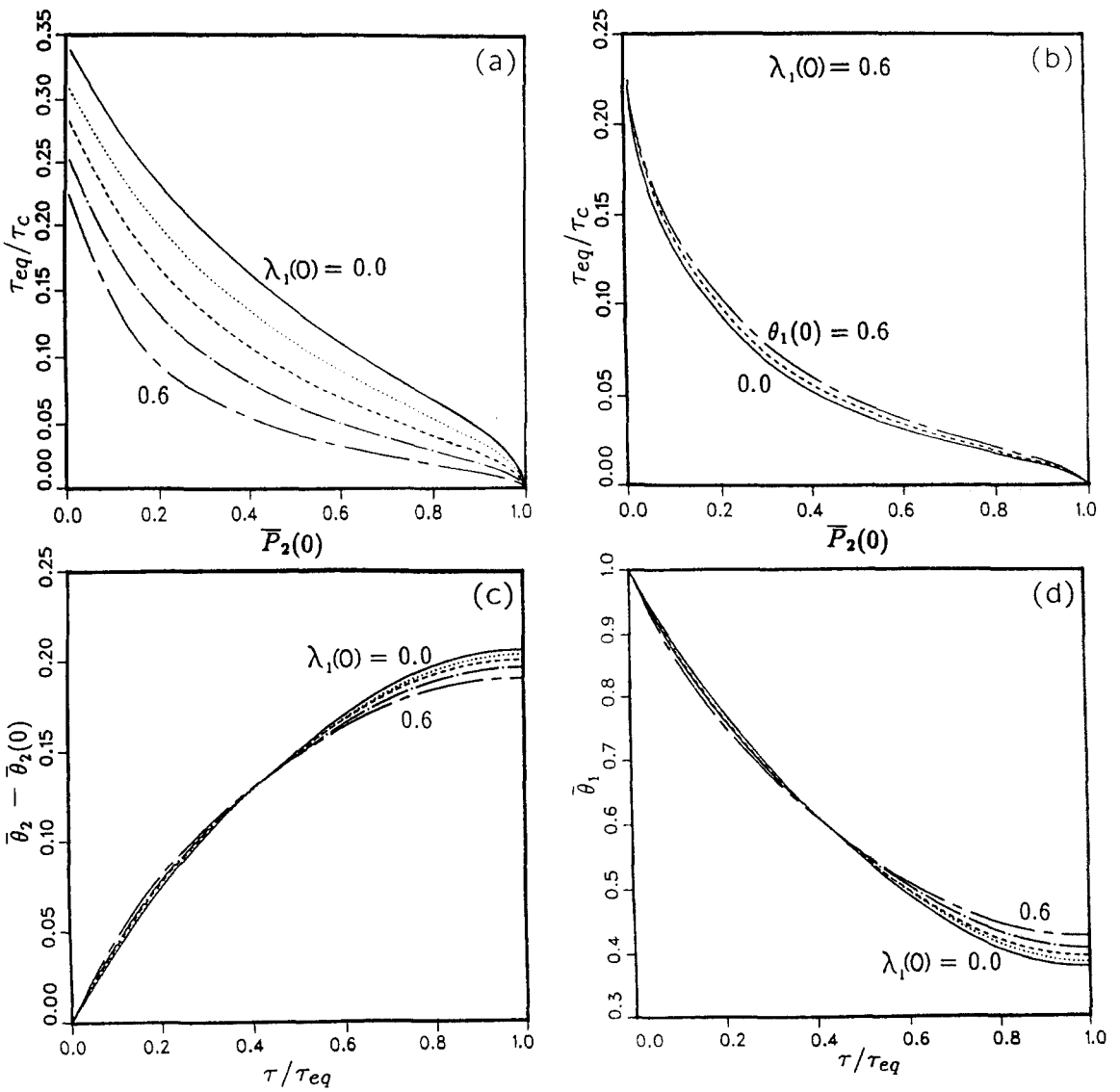

Figure 5—*continued opposite.*

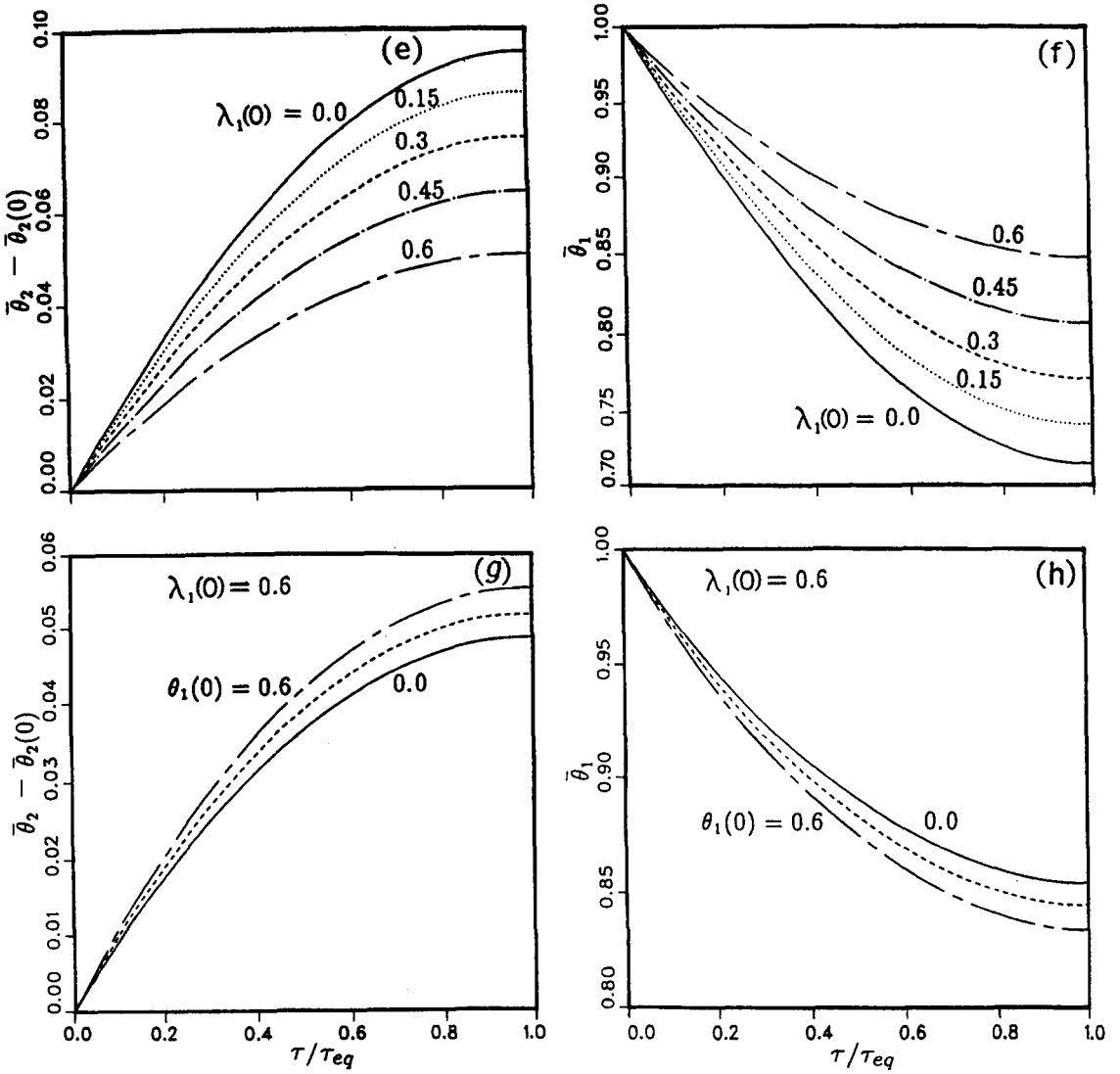

Figure 5. Solutions for $\bar{V}_2 = 3$. τ_{eq}/τ_c vs $\bar{P}_2(0)$: (a) $\bar{\phi}_2(0) = 1$; (b) $\bar{\phi}_2(0) \ll 1$. $\bar{\theta}_2 - \bar{\theta}_2(0)$ and $\bar{\theta}_1$ vs τ/τ_{eq}; (c, d) $\bar{\phi}_2(0) = 1$, $\bar{P}_2(0) = 0.01$; (e, f) $\bar{\phi}_2(0) = 1$, $\bar{P}_2(0) = 0.5$; (g, h) $\bar{\phi}_2(0) \leqslant 1$, $\bar{P}_2(0) = 0.5$.

sonic as well as initially subsonic cases. The corresponding results for $\bar{\theta}_1$ vs τ/τ_{eq} are given in figure 4(d) for the case where $\bar{P}_2(0) = 1/2$. Again, as for charging, the largest errors occur at small $\bar{P}_2(0)$ for τ_{eq}/τ_c rather than in the transient solution in terms of τ/τ_{eq}.

3.5. Numerical results for finite $\bar{V}_2$ and $\bar{\phi}_2(0) \neq 1$

Although approximate solutions for finite $\bar{V}_2$ are possible when $\bar{\phi}_2(0) = 1$ [and are similar to those for an ideal gas (Chenoweth 1974, sect. F)] they are not included here.

Before numerically investigating the parameter dependence for more general cases, an example with finite $\bar{V}_2$ is given for $\bar{\phi}_2(0) = 1$. Since the K_* and τ_* results showed that $\bar{V}_2 = 1$ is very similar to the $\bar{V}_2 \ll 1$ case, we give results for $\bar{V}_2 = 3$ in figure 5, where $\gamma_1 = 7/5$ and $\bar{T}_2(0) = 1$. Figure 5(a) gives τ_{eq}/τ_c vs $\bar{P}_2(0)$ with $\lambda_1(0)$ as the parameter, and the corresponding receiver and supply volume fractions are given vs τ/τ_{eq} in figures 5(c) and (d) for $\bar{P}_2(0) = 0.01$ and figures 5(e) and (f) for $\bar{P}_2(0) = 1/2$. The striking difference in these two cases is due to the substantial time spent with sonic flow when $\bar{P}_2(0) \ll 1$, where the effects of $\lambda_1(0)$ are both weaker and opposite to that present in the subsonic region. Also, since it was shown in the end-state section that the number of

independent parameters is minimized when $\bar{\phi}_2(0) = 1$, we compare some results in figure 5 where $\bar{\phi}_2(0) \ll 1$. In that case the additional parameters γ_G and $\theta_1(0)$ enter the problem. Figure 5(b) give τ_{eq}/τ_c vs $\bar{P}_2(0)$ for $\gamma_G = 5/3$ and $\lambda_1(0) = 0.6$ with $\theta_1(0)$ as the parameter. Figures 5(g) and (h) gives $\bar{\theta}_2 - \bar{\theta}_2(0)$ and $\bar{\theta}_1$ vs τ/τ_{eq} for $\bar{P}_2(0) = 0.5$ with the same parameters. It is clear that in this special case the dependence on $\theta_1(0)$ is relatively weak and of course it is even weaker for smaller $\lambda_1(0)$. In these plots $\theta_1(0) = 0$ and $\theta_1(0) = 0.6$ correspond to a high-pressure supply with small particle volume fraction and a low-pressure supply (ideal gas limit) with large particle volume fraction, respectively. These cases are not different when $\bar{\phi}_2(0) = 1$, but some small differences are clearly present when $\bar{\phi}_2(0) \ll 1$ and $\bar{V}_2 = 3$. Note that here ϕ_1 and δ_1 are arbitrary, so long as they produce $\gamma_1 = 7/5$.

It has already been shown, via end-state results, sonic conditions and transient solutions, that the discharge limit $\bar{V}_2 \gg 1$ depends on only γ_1, $\lambda_1(0)$ and $\bar{P}_2(0)$, and that there is increasing dependence on other parameters as $\bar{V}_2$ decreases. For this reason the remainder of the examples will be given for the $\bar{V}_2 \ll 1$ charging limit, in an attempt to show the maximum effects of the additional parameters. First we repeat the case shown in figures 5(b), (g) and (h) using $\bar{V}_2 \ll 1$ to show that, in this limit, the effects of $\theta_1(0)$ are much greater than shown previously for $\bar{V}_2 = 3$ and fixed $\lambda_1(0)$. These results are shown in figures 6(a) and (c). Physically the reason for the vast

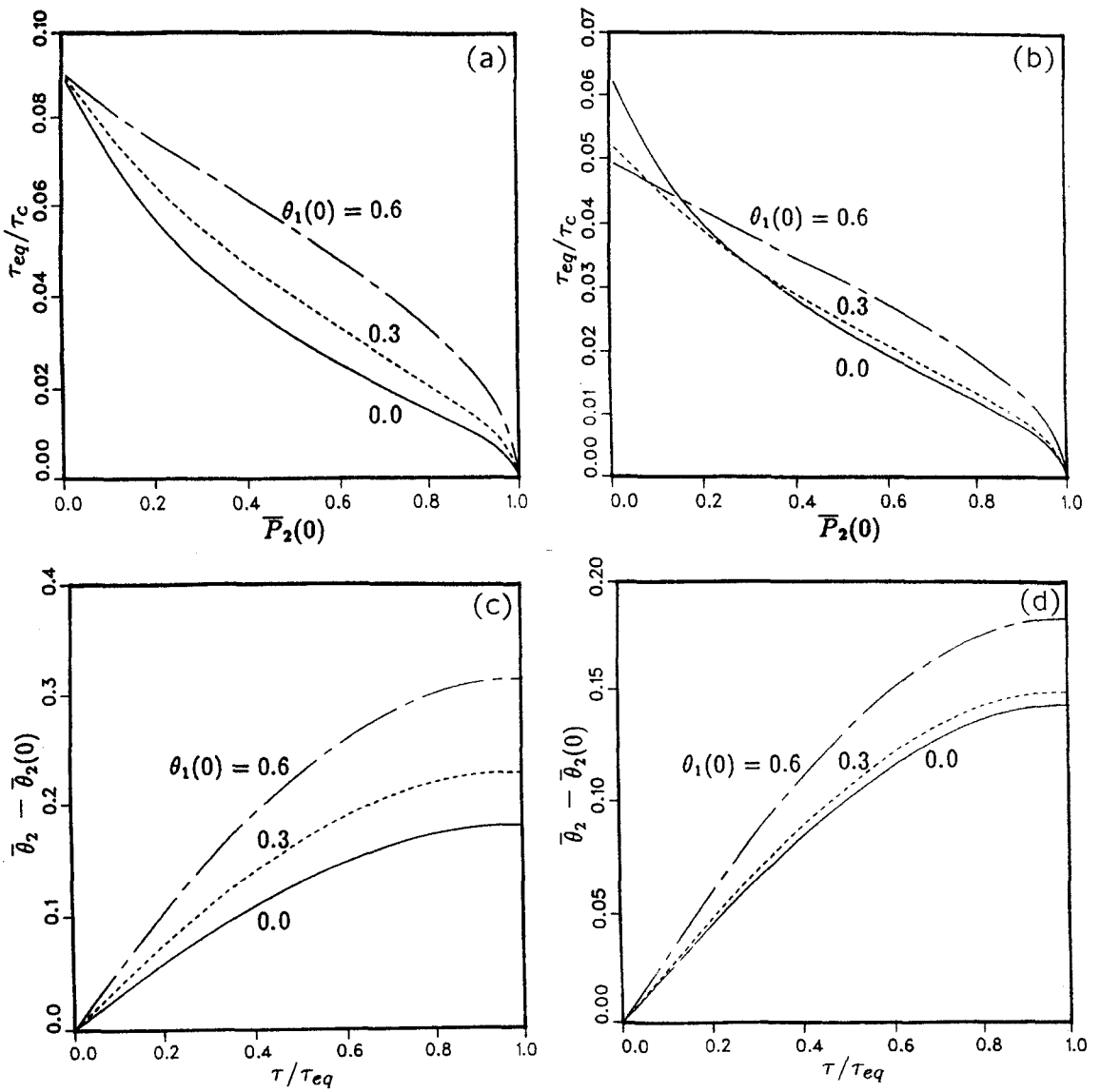

Figure 6. Charging solutions for $\bar{\phi}_2(0) \neq 1$. τ_{eq}/τ_c vs $\bar{P}_2(0)$: (a) $\bar{\phi}_2(0) \ll 1$, (b) $\theta_2(0) = 0.5$. $\bar{\theta}_2 - \bar{\theta}_2(0)$ vs τ/τ_{eq} with $\bar{P}_2(0) = 0.5$: (c) $\bar{\phi}_2(0) \ll 1$, (d) $\theta_2(0) = 0.5$.

difference in the parameter dependence for the charging and discharging limits is due to the effect of the receiver pressure changes. The additional parameters which allow the problem to distinguish between the molecule and particle volume fraction contributions to the combined parameter $\lambda_1(0)$ are not introduced into the discharging limit, since the receiver pressure is constant there. On the other hand, when the receiver pressure is changing rapidly, as for charging, the difference is maximized due to the fact that we have assumed that particles only affect pressure via volume displacement in contrast to the gas AN-EOS. Finally, to show the effects of having a substantial part of the receiver initially occupied by particles, the same problem is repeated with $\theta_2(0) = 1/2$ as the fixed parameter, rather than $\bar{\phi}_2(0) \ll 1$ which corresponded to $\theta_2(0) \ll 1$. These results are given in figures 6(b) and (d) and show reduced but still significant effects of $\theta_1(0)$ when $\lambda_1(0)$ is fixed.

As a final example we briefly look at the effects of material properties in situations where they can affect the results. First, we examine the case for $\bar{\phi}_2(0) \ll 1$ using a diatomic carrier gas rather than a monatomic one, as has been done to this point. The $\theta_1(0) = 0.3$ case shown in figures 6(a) and (c) for $\gamma_G = 5/3$ is compared with results for $\gamma_G = 7/5$ in figures 7(a) and (c), where obviously

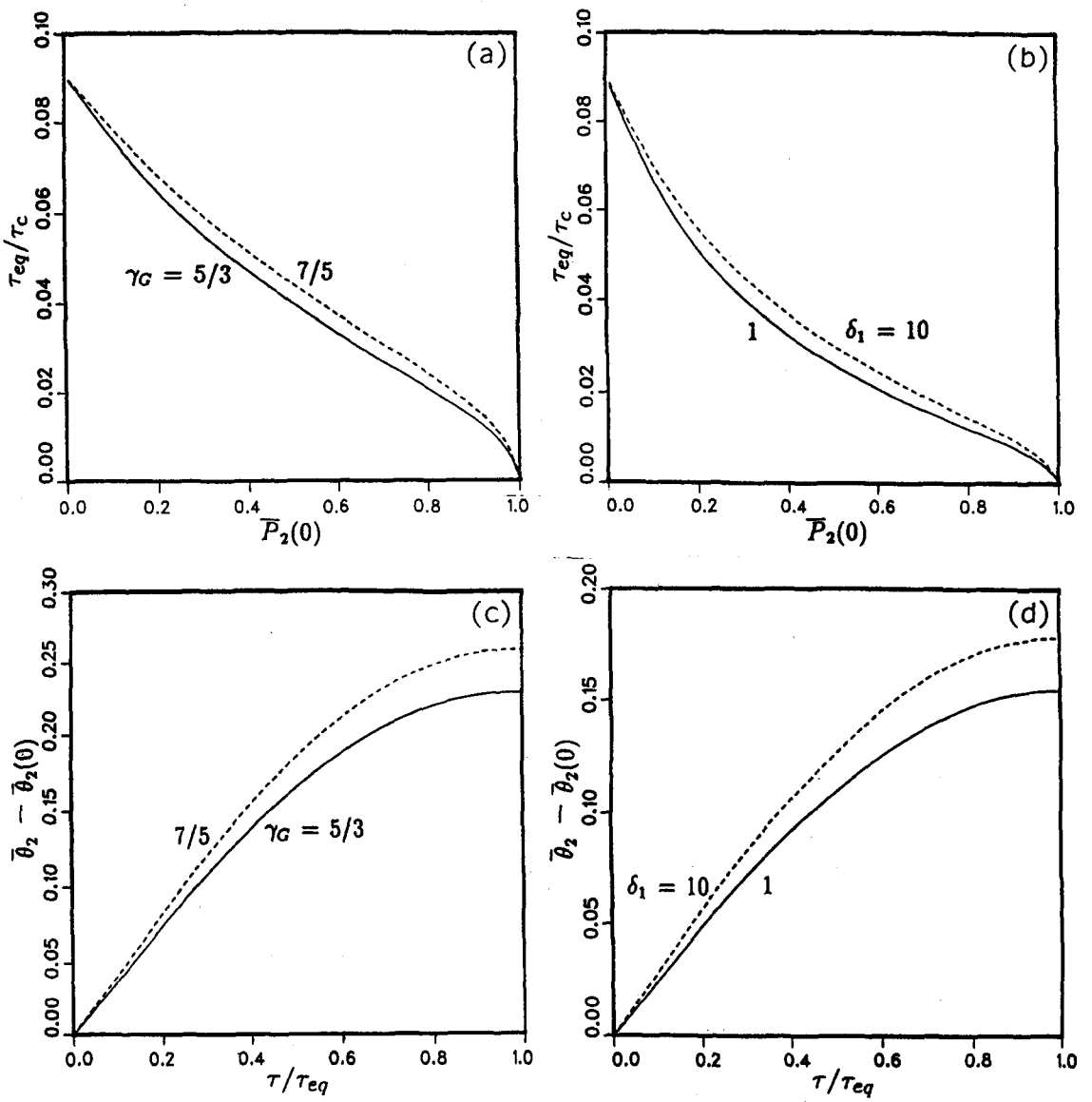

Figure 7. Effect of material properties on charging solutions. τ_{eq}/τ_c vs $\bar{P}_2(0)$: (a) $\bar{\phi}_2(0) \ll 1$ and $\gamma_G = 5/3$, 7/5; (b) $\bar{\phi}_2(0) = 2$ and $\delta_1 = 1$, 10. $\bar{\theta}_2 - \bar{\theta}_2(0)$ vs τ/τ_{eq} with $\bar{P}_2(0) = 0.5$: (c) $\bar{\phi}_2(0) \ll 1$ and $\gamma_G = 5/3$, 7/5; (d) $\bar{\phi}_2(0) = 2$ and $\delta_1 = 1$, 10.

δ_1 and ϕ_1 must combine with these γ_G values to produce $\gamma_1 = 7/5$. We see that the effects of γ_G are significant but not large. In addition, we show similar results for $\bar{\phi}_2(0) = 2$ in figures 7(b) and (d), since it was shown that when $\bar{\phi}_2(0) \neq 1$ and $\bar{\phi}_2(0)$ is also not negligible, then ϕ_1 or δ_1 can also independently affect the results. In this final case $\lambda_1(0) = 0.6$, $\theta_1(0) = 0.3$, $\gamma_1 = 7/5$, $\gamma_G = 5/3$ but $\delta_1 = 1$ ($\phi_1 = 2/7$) and $\delta_1 = 10$ ($\phi_1 = 1/26$) are compared. Again the effects are significant but not large.

It should be noted, that similar to the increase of $\bar{V}_2$ towards the discharge limit, the decrease of $\bar{P}_2(0)$ below K_* generally weakens the dependence on these additional parameters. The reason for this effect is that more time is spend with sonic flow, which depends on only γ_1 and $\lambda_1(0)$ with ϕ_1, δ_1 and γ_G being confined to the time scale factor τ_c and the mixture ratio of specific heats γ_1. At any rate, it appears that the more simple $\bar{\phi}_2(0) = 1$ results can often be used to estimate the behavior of more complex $\bar{\phi}_2(0) \neq 1$ cases which depend on more parameters.

4. CONCLUSIONS

The analysis of Part I for an ideal carrier gas has been extended to include non-ideal carrier gases which can be described adequately by an AN-EOS. These gases include helium, neon, hydrogen and their isotopes at low temperatures extending substantially below room temperature, as well as most other common gases at high temperatures.

It is shown that the expanding mixture or pseudo-fluid behaves as a modified AN gas which is pseudo-polytropic. This result occurs when the fluid is described in terms of the mixture ratio of specific heats and mixture volume fraction, each of which combine the individual effects of the particles and the gas molecules.

It is demonstrated that there are three cases where all results, including transient non-dimensional solutions, depend only on these mixture parameters (in addition to the usual initial vessel volume, pressure and temperature ratios where appropriate) with no explicit dependence on the individual contributions from particles or gas properties. One of these cases consists of the sonic flow portion of the transfer, if one exists. A simple, approximate sonic solution valid for most parameter ranges of physical interest, is given and compared to numerical results to show the mixture parameter dependence. Another case which does not distinguish between the separate contributions from the gas and the particles involves the single-fluid problem, where the initial mass fractions in the supply and the receiver are the same. Approximate expressions for the time of the end of sonic flow and the corresponding conditions there are given and are shown to describe the single-fluid problem over the entire range of parameters, including all vessel volume ratios. In this case the approximate subsonic flow solution is given and favorably compared to numerical results for the small volume ratio (charging) limit. The third case which involves the reduced number of mixture parameters is the large volume ratio (discharging) limit. The subsonic discharge results, including the approximate solution, are valid for all initial receiver mass fractions even if they are not the same as the supply, since the receiver conditions remain essentially unchanged, while the supply discharges to the receiver pressure level.

In the subsonic regime for finite $\bar{V}_2$, with the exception of the special single-fluid case, a numerical solution is necessary when the changing receiver pressure (and parameters that it is a function of) enters in the differential problem. Results are given which show the effects of parameters describing individual particle and gas contributions in instances not covered by the three special cases. The dependence on the additional parameters decreases as the receiver to supply volume ratio increases and as the initial receiver to supply pressure ratio decreases below the critical value. However, the results show that often the more simple single fluid results can be used to adequately estimate the behavior of the more complex cases which depend on the additional parameters.

Finally, the hierarchy of controlling independent dimensionless parameters, varying from as few as 6 to as many as 10 depending on the nature of the problem and how it is specified, has been established by means of the end-state analysis and limiting solutions given in the Appendix. The limiting solutions also reveal the conditions under which a significant mass defect can exist at pressure equilibrium, as well as when the adiabatic pressure equilibrium can be significantly different from that finally reached at thermal equilibrium.

Acknowledgement—This work was performed in part under the auspices of the U.S. Department of Energy by Sandia National Laboratories, Livermore, CA, under Contract No. DE-AC04-76DP 00789.

REFERENCES

CHENOWETH, D. R. 1974 Gas transfer analysis: sections A–F. Sandia National Labs Reports (A) SAND74-8211, (B) SAND74-8212, (C) SAND74-8213, (D) SAND74-8214, (E) SAND74-8215 and (F) SAND74-8216.

CHENOWETH, D. R. 1983 Gas transfer analysis: section H—real gas results via the van der Waals equation of state and virial expansion extensions of its limiting Abel–Noble form. Sandia National Labs Report SAND83-8229.

CHENOWETH, D. R. & PAOLUCCI, S. 1989 On pressure change occurring during gas mixing. *Am. J. Phys.* **57**, 463–465.

CHENOWETH, D. R. & PAOLUCCI, S. 1990a Compressible flow of a two-phase fluid between finite vessels—I. Ideal carrier gas. *Int. J. Multiphase Flow* **16**, 1047–1069.

CHENOWETH, D. R. & PAOLUCCI, S. 1990b Compressible flow of a multiphase fluid between two vessels: Part I—ideal carrier gas. Sandia National Labs Report SAND90-8486.

HIRSCHFELDER, J. O., CURTISS, C. F. & BIRD, R. B. 1967 *Molecular Theory of Gases and Liquids*. Wiley, New York.

VAN WYLEN, G. J. & SONNTAG, R. E. 1973 *Fundamentals of Classical Thermodynamics*, 2nd edn. Wiley, New York.

APPENDIX

A number of limiting solutions to [14] for the adiabatic end-state are given below.

1. $\gamma_1 \to 1$ (Isothermal Limit)

There are three independent ways to cause $\gamma_1 \to 1$: $\gamma_G \to 1$, $\phi_1 \to 1$ and $\phi_1 \delta_1 \gg 1$. When $\gamma_1 \to 1$ (supply vessel isothermal), [14] becomes quadratic in $\bar{\theta}_1(t_{eq})$. The case $\gamma_G \to 1$ results in the trivial no flow limit $\bar{\theta}_1(t_{eq}) \to 1$. The no flow limit also occurs whenever $\bar{P}_2(0) \to 1$, $\bar{V}_2 \to 0$ or $\theta_2(0) \to 1$. For $\phi_1 \to 1$ or $\phi_1 \delta_1 \gg 1$ the non-trivial solution $\bar{\theta}_1(t_{eq}) = \bar{\theta}_1(\infty)$ results, where $\bar{\theta}_1(\infty)$ is given by [9]. In this case

$$\bar{P}_1(t_{eq}) = \frac{\bar{P}(\infty)}{\bar{T}(\infty)}, \qquad [A.1]$$

which is the same as given by [7] only when $\bar{T}(\infty) = 1$.

2. $V' \ll 1$ (Charging Limit)

When the initial receiver gas volume is much smaller than the initial supply gas volume, the supply conditions will remain essentially unchanged during the charging of the receiver to the supply pressure level, so that $\bar{P}_1 \approx 1$ and $\bar{\theta}_1 \approx 1$.

The conditions in the receiver do change and can be investigated via [12] and [13] and [I.30]–[I.33] if the limiting results are carefully derived. The procedures and results are similar to those of a pure gas [see Chenoweth (1974, sects C and D)]. When $\phi_2 = \phi_1$ and using $\bar{P}_2(t_{eq}) = 1$,

$$\bar{\theta}_2(t_{eq}) = \bar{\theta}_2(0)\left\{1 + \frac{\bar{T}_2(0)}{\gamma_1 \bar{P}_2(0)}[1 - \lambda_1(0)][1 - \bar{P}_2(0)]\right\} \qquad [A.2]$$

and

$$\bar{T}_2(t_{eq}) = \frac{\gamma_1 - \lambda_1(0)[1 - \bar{P}_2(0)]}{1 + \bar{P}_2(0)\left[\frac{\gamma_1}{\bar{T}_2(0)} - 1\right] - \lambda_1(0)[1 - \bar{P}_2(0)]}. \qquad [A.3]$$

When the receiving vessel is initially evacuated $\bar{T}_2(t_{eq}) \to [\gamma_1 - \lambda_1(0)]/[1 - \lambda_1(0)]$. This limit gives the maximum effect of compressive heating during the charging process, which for a pure ideal gas reduces to the well-known result of γ_G. Clearly, temperatures exceeding the pure ideal gas limit are possible when $\lambda_1(0) \neq 0$. Also notice from [A.2] that when an evacuated vessel, initially containing

no particles, is used to rapidly draw a sample from its surroundings, the sample volume fraction may be less than that of its surroundings by a factor as large as $\gamma_1 \to \infty$, since

$$\bar{\theta}_2(t_{eq}) \to \frac{1}{\gamma_1} + \bar{\theta}_2(0)\left[1 - \frac{\theta_1(0)}{\gamma_1}\right]$$

as $\bar{P}_2(0) \to 0$. Therefore, one can have a substantial sampling error unless thermal equilibrium is also reached.

3. $V' \gg 1$ (Discharging Limit)

In this limit the receiver conditions remain essentially unchanged, so that the supply discharges to the receiver pressure level. Therefore, from [12] or [14] we obtain the supply volume fraction at the adiabatic pressure equilibrium $\bar{P}_1(t_{eq}) = \bar{P}_2(0)$:

$$\bar{\theta}_1(t_{eq}) = \{\lambda_1(0) + [1 - \lambda_1(0)]\bar{P}_2(0)^{-1/\gamma_1}\}^{-1}. \quad [A.4]$$

For a pure ideal gas this limit recovers the results of Chenoweth (1974, sect. E, 1983).

4. $\alpha = \beta$ (Single Fluid or Negligible Particle Heat Capacity Limit)

Another solution of [14] occurs when $\alpha = \beta$, giving

$$\bar{\theta}_1(t_{eq}) = \{\lambda_1(0) + [1 - \lambda_1(0)]\bar{P}_1(t_{eq})^{-1/\gamma_1}\}^{-1}, \quad [A.5]$$

where

$$\bar{P}_1(t_{eq}) = \frac{\lambda_1(0)\bar{P}_2(0) + [1 - \lambda_1(0)]\bar{T}_2(0) + \bar{V}_2\bar{P}_2(0)\bar{T}_2(0)}{\lambda_1(0)\bar{P}_2(0) + [1 - \lambda_1(0)]\bar{T}_2(0) + \bar{V}_2\bar{T}_2(0)}; \quad [A.6]$$

then $\bar{P}_1(t_{eq}) = \bar{P}(\infty)$ only if $\bar{T}(\infty) = \bar{T}_2(0) = 1$. This special solution can occur in three ways:

(a) receiver initially evacuated with no particles, $\bar{P}_2(0) = 0$, $\theta_2(0) = \phi_2(0) = 0$;
(b) mass fraction of particles the same in each vessel (single fluid) $\phi_1 = \phi_2(0)$; or
(c) particle heat capacity negligible compared to that of the gas, $\delta_1 \ll 1$, $\gamma_1 \to \gamma_G$.

Obviously cases (a) and (b) both result in single-fluid transfer problems. For case (a) $\alpha = \beta = 0$, while for cases (b) and (c) we have

$$\alpha = \beta = \rho'\left[\frac{1 - \theta_2(0)}{1 - \theta_1(0)}\right]. \quad [A.7]$$

5. The Mass Defect

In the limiting solutions given above, $\bar{\theta}_1(t_{eq}) \neq \bar{\theta}_1(\infty)$ except for very special cases. In order to examine the magnitude of the difference, a mass defect parameter is defined analogous to that defined by Chenoweth (1974, sect. A, 1983):

$$\Delta \equiv \frac{\bar{\theta}_1(t_{eq}) - \bar{\theta}_1(\infty)}{1 - \bar{\theta}_1(\infty)}. \quad [A.8]$$

Since $\bar{\theta}_1 = \bar{\rho}_1$, this parameter represents the maximum fraction of the mass transferred at thermal equilibrium, which may be retained in the supply when pressure equilibrium is first reached. This mass defect is due to departures from thermal equilibrium and can be bounded in some cases. For example, using [9] and [A.5] in [A.8] when $\bar{T}_2(0) = 1$ so that $\bar{P}_1(t_{eq}) = \bar{P}(\infty)/\bar{T}(\infty)$ when $\alpha = \beta$, we get

$$\Delta = \frac{\bar{P}_1(t_{eq})^{1/\gamma_1} - \bar{P}_1(t_{eq})}{[1 - \bar{P}_1(t_{eq})]\{1 - \lambda_1(0)[1 - \bar{P}_1(t_{eq})^{1/\gamma_1}]\}}, \quad [A.9]$$

which is bounded by

$$\Delta_0 \leqslant \Delta \leqslant \Delta_1 = \Delta_0\{\bar{P}_1(t_{eq})^{-1/\gamma_1} + \lambda_{G1}(0)[1 - \bar{P}_1(t_{eq})^{-1/\gamma_1}]\}. \quad [A.10]$$

The subscript on Δ refers to the values of $\theta_1(0)$. That is, for all $0 \leqslant \theta_1(0) \leqslant 1$, Δ is always greater than that of pure gas ($\theta_1(0) = 0$) for any given $\bar{P}_1(t_{eq})$. For $\lambda_1(0) \leqslant 1/2$, a smaller upper bound can be obtained using

$$\theta_1(0) \leqslant \psi \equiv \left[\frac{\frac{1}{2} - \lambda_{G1}(0)}{1 - \lambda_{G1}(0)}\right]$$

in the form

$$\Delta \leqslant \Delta_\psi \leqslant 1 - \frac{1}{\gamma_1}. \qquad [A.11]$$

The value $1 - 1/\gamma_1$ is approached for all $\lambda_1(0)$, when $\bar{P}_1(t_{eq})$ (given by [A.6]) approaches unity; clearly this is possible only when $V' \ll 1$ or $\bar{P}_2(0) \to 1$. When $\gamma_1 \to \gamma_G$ and $V' \to \bar{V}_2$, the results agree with those for a pure gas given by Chenoweth (1974, sect. A, 1983). For $\psi \leqslant \theta_1(0) < 1$ a maximum value occurs when $d\Delta/d\bar{P}_1(t_{eq}) = 0$ in the interval $0 < P_1(t_{eq}) \leqslant 1$ with the value $1 - 1/\gamma_1 \leqslant \Delta_{max} < \Delta_1 \leqslant 1$, where unity is approached by Δ_1 as $\bar{P}_1(t_{eq}) \to 0$. Expressions [A.9] and [A.11] are valid whenever $V' \gg 1$, $\gamma_1 \to 1$ or $\alpha = \beta$ with $\bar{T}_2(0) = 1$, as separate cases or in combination, and then $\bar{P}(\infty) = \bar{P}_1(t_{eq})$ if $\bar{T}(\infty) = 1$. The results for Δ when $\alpha = \beta$ and $P_r \equiv 1$ (see definition [A.12] below) are given in figure 6 of Chenoweth & Paolucci (1990b) and are valid for $\lambda_{G1}(0) \neq 0$, provided the parameter $\theta_1(0)$ labeling the curves there is replaced by $\lambda_1(0)$.

It is of interest to examine the mass defect (as defined by [A.8]), and the pressure ratio

$$P_r \equiv \frac{\bar{P}_1(t_{eq})}{\bar{P}(\infty)} \qquad [A.12]$$

using the numerical solution of [14] when $\alpha \neq \beta$, $\gamma_1 \neq 1$ and V' is finite, to determine if significant deparatures from the special cases can exist. For such general cases, if $\bar{T}(\infty)$ is included, 10 independent parameters can affect the results for Δ and P_r. The detailed comparisons of that study using an ideal carrier gas $\lambda_{G1}(0) \ll 1$ are given in Chenoweth & Paolucci (1990b). Space restrictions do not permit general results to be given here for the AN gas case; however, the transient results as $t \to t_{eq}$ do illustrate the end-state solutions just derived. The behavior resulting if $P_r \neq 1$ is analogous in some respects to that found for ideal gas mixing involving different temperatures and different internal molecular structure (see Chenoweth & Paolucci 1989).